TYPE SYNTHESIS AND KINEMATIC ANALYSIS OF TRANSLATIONAL PARALLEL MANIPULATORS

Wei Wei

Department of Mechanical Engineering
McGill University, Montréal

April 2005

A Thesis submitted to the Faculty of Graduate Studies and Research
in partial fulfilment of the requirements for the degree of
Master of Engineering

ABSTRACT

This thesis treats type synthesis and kinematic analysis of translational parallel manipulators (TPMs) from a group theoretical point of view.

For the TPM type synthesis, based on displacement group theory (DGT), TPM leg motion is represented by a series of displacement subgroups. For symmetrical three-legged TPMs, three categories are classified and a total of 90 architectures are proposed. For asymmetrical three-legged TPMs, 13 cases of possible leg combinations are presented and some possible constructions of TPMs are shown. The advantages of DGT in mechanism synthesis are described.

For the kinematic analysis of symmetrical TPMs, geometric elements are employed to denote the workspace of different leg links. Solutions of the inverse and direct kinematics of a certain example are obtained. Moreover, the proposed approach is applied to a class of TPMs, and the corresponding geometric representations are listed. The applicability of the proposed approach is discussed as well.

This thesis provides a theoretical approach to design TPMs and analyze their kinematics for practical applications.

RÉSUMÉ

Cette thèse porte sur l'aspect théorique de la synthèse structurelle et l'analyse cinématique des manipulateurs parallèles à mouvements de translation (TPMs).

La synthèse structurelle des TPM est basée sur la théorie des groupes de déplacement (DGT) où chaque patte d'un TPM est représentée par une série de sous-groupements de déplacement. Les TPMs symétriques à trois pattes sont classés en trois catégories et un total de quatre-vingt-dix architectures sont proposées. Dans le cas des TPMs asymétriques à trois pattes, treize combinaisons de membrures sont présentés et certaines parties de la construction de ces TPMs sont illustrés. De plus, les avantages du DGT appliqué à la synthèse des mécanismes sont décrits.

Concernant l'analyse cinématique des TPMs symétriques, des éléments de géométrie sont employés pour exprimer l'espace de travail des différentes membrures de chaque patte. Certains exemples de problèmes géométriques directs et inverses sont également résolus et présentés. De plus, l'approche proposée est appliquée pour une classe de TPMs et les représentations géométriques correspondantes sont énumérées. La faisabilité de l'approche proposée est de plus discutée.

Cette thèse fourni une approche théorique de concevoir TPMs et analyser leur cinématique pour des applications pratiques.

ACKNOWLEDGEMENTS

First of all, I would like to thank my supervisor, Professor Zsombor-Murray, for enlightenment and guidance during my master program at McGill University. He led me into the field of robotics and inspired me with insightful ideas. His knowledge and humour, of which I have yet a lot to learn, deeply impressed me.

I would also like to thank my colleagues at the Centre for Intelligent Machines (CIM) for their advice and help while I work on my thesis. Thanks to their precious suggestions, I can better perform my study and research. Their friendship is greatly supportive to me in study and in day to day life.

Moreover, I thank the Department of Mechanical Engineering and CIM for providing a research environment from which I have greatly benefited.

Finally, I must thank my parents. Their long-term support and encouragement helped me to successfully overcome difficulties in my study and life. Each step of my development is dependent upon their love. I can never thank them enough.

TABLE OF CONTENTS

LIST OF FIGURES

LIST OF TABLES

CHAPTER 1

Introduction

This thesis is a comprehensive investigation of translational parallel manipulators (TPMs), including both type synthesis and kinematic analysis. Based on displacement group theory (DGT), the synthesis procedure is quite easy to follow and the results present all possible three-legged TPMs. With line geometry, the direct and inverse kinematics of TPMs can be simplified to geometric problems and analyzed in a unified fashion. These two methodologies are applicable to other problems in mechanism synthesis and analysis.

1.1. Thesis Subject Development

Parallel-kinematics machines (PKMs) generally consist of a moving platform connected to a fixed base by several kinematic chains, called the legs. Typically, though not always, each leg has one actuated joint. Therefore, the number of degrees of freedom (dof) of such a PKM is equal to the number of legs. PKMs are reputed to have several advantages over their serial counterpart, like high structural rigidity, increased load capacity and higher accuracy. The Stewart platform (Stewart, 1965) is a classical example of PKMs, which has six dofs and all the linear actuators are under pure axial forces. Variations of the Stewart platform have been proposed. Kohli *et al.* (1988) designed a six-dof parallel manipulator that utilizes base-mounted rotary-linear actuators; Pierrot *et al.* (1991) developed the high-speed "Hexa" six-dof parallel

manipulator; and Tahmasebi and Tsai (1994) proposed a six-dof parallel manipulator with three inextensible limbs. However, existing six-dof PKMs have drawbacks such as complex direct kinematics, small workspace, and complications due to universal and spherical joints, especially in quasi-coincident ones.

Parallel manipulators with fewer than six dofs have been developed to overcome some disadvantages. Their simpler architectures and better performances in certain applications have stimulated considerable research interest. TPMs are one family of reduced-dof PKMs. The end effector (EE) of TPMs can perform translations in all directions but provides no change in rotation. A special application of TPMs is in the fields of automated assembly where component orientation must remain fixed under manipulation or where orientation is of no concern like with a uniform sphere. Since the first TPM, the Delta robot (Clavel, 1988), was produced in the 1980's, researchers have investigated a number of TPM designs, hence TPMs of various architectures have been proposed, designed and built. Tsai *et al*. (1996) configured a TPM with a structure similar to the Delta robot. Chablat and Wenger (2003) developed a three-dof TPM for machining applications, the Orthoglide. Kong and Gosselin (2002) performed kinematics and singularity analysis for a three-$\underline{\text{C}}$RR TPM, where $\underline{\text{C}}$ means that the translational dof of the cylindrical pair is actuated. Kim and Tsai (2003) built the Cartesian Parallel Manipulator, called CPM, whose leg is a PRRR kinematic chain, where P stands for a prismatic joint and R is a revolute joint. Carricato and Parenti-Castelli (2003) developed a family of three-dof TPMs and did both inverse and direct position analysis. Tsai and Joshi (2001) compared four TPM architectures and proposed a design for hybrid kinematic machines.

In accordance with the proposed individual TPM architectures, this thesis presents a systematic approach to synthesize TPMs based on DGT. Other researchers have also attempted to design TPMs from a theoretical point of view. For example, Di Gregorio (2002) presented a family of TPMs with five-dof leg architectures; Carricato and Parenti-Castelli (2002) proposed singularity-free fully-isotropic TPMs by classifying the entire TPM family into three subcategories; and Kong and Gosselin

(2004) did type synthesis of TPMs based on screw theory and derived the whole class of possible leg architectures, as well as the TPM structures. However, the author believes that use of DGT renders the synthesis procedure quite straightforward and easier to follow. Synthesis based on DGT can generate all possible structures of the three-legged TPM family. Moreover, this method can exempt one from frustrating mathematical concepts and tedious derivations, which is a main concern in mechanism synthesis, since simpler synthesis procedures mean more efficient design and extends opportunity to examine a wider variety of alternatives. This approach was used by Hervé (1991, 1999) to perform mechanism design including architecture synthesis of several representative TPMs, and by Angeles (2004) to carry out qualitative synthesis of PKMs. The main contribution of this thesis is to produce comprehensive results.

Regarding the direct and inverse kinematics of TPMs, algebraic and projective line geometry elements are used herein to represent the workspace of different links. By intersecting these geometric graphs, kinematics solutions can be obtained in a unified fashion. A detailed analysis of the Delta robot has been given by Zsombor-Murray (2001), using a similar approach. In contrast, a different TPM architecture, with prismatic pairs instead of revolute pairs coupled to the base, is analyzed. Moreover, the idea to apply the algebraic geometric method to formulate and algebraically solve kinematics problems of TPMs in a general way is exposed. Due to similarities in structure and movement characteristics among TPMs, a common kinematics algorithm can be very helpful to analyze a variety of mechanisms, and can thus simplify the solution procedure. That is another contribution of this thesis.

1.2. Thesis Overview

In Chapter 2, relevant mathematical concepts and theories are introduced. These concepts will be applied in subsequent chapters.

Chapters 3 and 4 describe the procedure of TPM type synthesis. Chapter 3 focuses on leg architecture synthesis. Chapter 4 deals mainly with building the whole

three-legged TPM family structure, including symmetrical and asymmetrical architectures. Also, examples are given in Chapter 4 to show how DGT is applied to mechanism synthesis.

Chapters 5 and 6 present the kinematic analysis of TPMs using geometric elements. Chapter 5 treats a specific example and performs detailed analysis of its direct and inverse kinematics. Chapter 6 applies this approach in a more general way and summarizes the applicability of this method to a class of TPMs. Again, examples are given in Chapter 6 to demonstrate the effectiveness of the proposed approach.

Finally, Chapter 7 summarizes main contributions of this research work and anticipates broader applications in future mechanism synthesis and analysis.

CHAPTER 2

Mathematical Background

In this chapter, some relevant mathematical theories and concepts are recalled. These will be used later. Subsection 2.1 introduces dual quaternions. Subsection 2.2 recalls the group theory and displacement subgroups. Subsection 2.3 describes the duality of point and line in the plane, as well as Plücker coordinates.

2.1. Dual Quaternions

Quaternions are members of a noncommutative division algebra. Similar to the complex numbers being representable as a sum of real and imaginary parts, a quaternion can also be written as a linear combination of real and imaginary parts (Zsombor-Murray, 1998), in which the quaternion is put into a vector format.

$$\mathbf{Q} = c_0 + c_1 i + c_2 j + c_3 k = \begin{bmatrix} c_0 \\ c_1 \\ c_2 \\ c_3 \end{bmatrix} \tag{2.1}$$

A dual quaternion includes both dual and real parts. A general expression of a dual quaternion is given as well.

$$\mathbf{Q}_d = (c_0 + \epsilon q_0) + [(c_1 + \epsilon q_1)i + (c_2 + \epsilon q_2)j + (c_3 + \epsilon q_3)k] = \begin{bmatrix} c_0 + \epsilon q_0 \\ c_1 + \epsilon q_1 \\ c_2 + \epsilon q_2 \\ c_3 + \epsilon q_3 \end{bmatrix} \tag{2.2}$$

The expression in Eq. (2.2) separates the dual quaternion into a dual scalar and a dual vector. Sometimes, a dual quaternion is also divided into real and dual parts, *i.e.*, two quaternions, one of which is multiplied by the dual unit ϵ where $\epsilon^2 = 0$.

$$\mathbf{Q}_d = \mathbf{Q} + \epsilon\mathbf{Q}_\epsilon = \begin{bmatrix} c_0 \\ c_1 \\ c_2 \\ c_3 \end{bmatrix} + \epsilon \begin{bmatrix} q_0 \\ q_1 \\ q_2 \\ q_3 \end{bmatrix} \tag{2.3}$$

where

$$\mathbf{Q} = \begin{bmatrix} c_0 \\ c_1 \\ c_2 \\ c_3 \end{bmatrix} = \begin{bmatrix} \cos(\phi/2) \\ \cos(\alpha)\sin(\phi/2) \\ \cos(\beta)\sin(\phi/2) \\ \cos(\gamma)\sin(\phi/2) \end{bmatrix} \tag{2.4}$$

and

$$\mathbf{Q}_\epsilon = \frac{1}{2} \begin{bmatrix} 0 \\ a_1 \\ a_2 \\ a_3 \end{bmatrix} \begin{bmatrix} c_0 \\ c_1 \\ c_2 \\ c_3 \end{bmatrix} = \frac{1}{2} \begin{bmatrix} -(a_1c_1 + a_2c_2 + a_3c_3) \\ (a_1c_0 + a_2c_3 - a_3c_2) \\ (a_2c_0 + a_3c_1 - a_1c_3) \\ (a_3c_0 + a_1c_2 - a_2c_1) \end{bmatrix} \tag{2.5}$$

Note that the operation rule of the multiplication of two quaternions is that each element in one quaternion should be multiplied to all elements of the other. It is the same as the multiplication of two polynomials. The operation rules of the imaginary

units are summarized as

$$\begin{aligned} & i \cdot i = j \cdot j = k \cdot k = -1 \\ & i \cdot j = k,\ j \cdot k = i,\ k \cdot i = j \\ & i \cdot j = -j \cdot i,\ j \cdot k = -k \cdot j,\ k \cdot i = -i \cdot k \end{aligned} \tag{2.6}$$

Note that i, j and k are notions of three mutually orthogonal imaginary units.

2.2. Group Theory

In algebra, a group is a set G of elements related by a binary operation "$*$" with four properties:

1) If a and $b \in G$, then $a * b \in G$;

2) If a, b and $c \in G$, then $a * (b * c) = (a * b) * c$;

3) G contains an element σ called the identity of G under "$*$", such that $a * \sigma = \sigma * a = a$;

4) For every $a \in G$, there exists an element a^{-1}, called the inverse of a under "$*$" such that $a * a^{-1} = a^{-1} * a = \sigma$.

In order, the four properties are called closure, associativity, idempotence and inversibility, respectively.

A subgroup G_s of a given group G is a set of objects such that:

1) $\forall\ a \in G_s$, then $a \in G$;

2) $\exists\ b \in G$, where $b \notin G_s$;

3) G_s satisfies the four group properties with respect to the binary operation "$*$".

Rigid-body displacements constitute a group with subgroups. If the elements of a set D are rigid-body displacements, then a binary operation "$*$" of displacements can be defined as the concatenation of some: As the body first undergoes a displacement

d_a, taking the body from pose B_0 to pose B_a, and then a displacement d_b, taking the same body from pose B_a to pose B_b, successively, it is apparent that the concatenation of the two displacements, $d_a * d_b$, is also a rigid-body displacement (Angeles, 2003).

Using dual quaternions, subgroup properties of rigid-body displacements can be better illustrated from an algebraic point of view. In accordance with rigid-body displacements, in Eq. (2.4), ϕ denotes the angle of rotation undergone by the rigid body about its axis of rotation; α, β and γ are angles formed between the axis of rotation and coordinate axes. Therefore, the real part of a dual quaternion completely represents rotations of a rigid body in three-dimensional space. In Eq. (2.5), a_1, a_2 and a_3 are three components of the vector representing a rigid-body displacement, and the dual part of a dual quaternion represents the translational motion of a rigid body. Defined in this way, it is clear that by setting certain elements of the dual quaternion to zero, certain displacements can be represented. For example, by setting

$$c_1 = c_2 = a_3 = 0$$

accordingly, one obtains

$$c_1 = c_2 = q_0 = q_3 = 0$$

which represents the planar motion, and if

$$a_1 = a_2 = a_3 = 0$$

accordingly, one obtains

$$q_0 = q_1 = q_2 = q_3 = 0$$

which represents pure rotation in all directions. Besides, $c_1 = c_2 = c_3 = 0$ represents the spatial translation, and $c_1 = c_2 = 0$ represents the Schönflies motion. Accordingly, all possible displacements in three-dimensional space can be represented by dual quaternions.

Now the subgroup properties of a general displacement can be examined systematically. For example, one can define two displacements with different parameters.

Through operations, it can be verified that a combination of the two displacements is still a displacement itself, namely that it satisfies the closure condition. Similarly, the other three conditions must be met as well. Therefore, practically, one can say a general displacement in three-dimensional space meets the conditions of a group, and hence, it forms a group $\{D\}$.

A subgroup $\{D_s\}$ of the group $\{D\}$ is itself a group of displacements, but generally lacks some properties of the general one. Since a subgroup is confined to the same four conditions, one can determine whether a certain displacement forms a subgroup. For example, the planar motion forms a planar subgroup since it concurrently satisfies the four conditions, and it is contained in the entire displacement group $\{D\}$. However, a combination of two rotations with non-parallel axes does not form a subgroup, because such a combination violates the closure condition.

Using this approach, one can comprehensively examine displacement subgroups and obtain all existing ones. A more detailed description and application of displacement subgroups will be given in Chapter 3 in order to synthesize the TPM leg architectures.

2.3. Point, Plane and Line

2.3.1. Points and Planes in Homogeneous Vector Space. In a homogeneous four-dimensional vector space, point position vectors are represented by four component magnitudes, $P(w : x : y : z)$. A plane is similarly represented by $p(W : X : Y : Z)$. With homogeneous coordinates, it is convenient to denote points at infinity by setting $w = 0$, and to denote a plane passing through the origin by setting $W = 0$ (Zsombor-Murray, 1996).

2.3.2. Plücker Line Coordinates. Now we consider the line on two given points $(w_i : x_i : y_i : z_i)$ $(i = 1, 2)$ expressed by a 4×4 determinant of a rank-2 matrix;

$$\begin{bmatrix} w_1 & x_1 & y_1 & z_1 \\ w_2 & x_2 & y_2 & z_2 \end{bmatrix}$$

expanding the determinant on 2×2 minors and cofactors yields

$$\mathcal{L}_r\{(w_1x_2 - w_2x_1) : (w_1y_2 - w_2y_1) : (w_1z_2 - w_2z_1) : (y_1z_2 - y_2z_1) :$$
$$(z_1x_2 - z_2x_1) : (x_1y_2 - x_2y_1)\} = \{p_{01} : p_{02} : p_{03} : p_{23} : p_{31} : p_{12}\}$$

The first three coordinates are the line direction numbers and the last three are the components of the moment of these numbers about O, the origin of the reference frame. Obtained by expanding on two given points, the Plücker coordinates are called *radial*. These coordinates are subject to conditions

$$p_{01}^2 + p_{02}^2 + p_{03}^2 + p_{23}^2 + p_{31}^2 + p_{12}^2 \neq 0$$

and

$$p_{01}p_{23} + p_{02}p_{31} + p_{03}p_{12} = 0$$

thereby restricting the line to its required four free parameters rather than six implied by its homogeneous coordinates.

Similarly, if one expands a pair of plane coordinates, the resulting Plücker coordinates are $\mathcal{L}_a\{P_{01} : P_{02} : P_{03} : P_{23} : P_{31} : P_{12}\}$, which are called *axial*. The first three coordinates are the moment components of the line with direction numbers corresponding to the last three. If a pair of points and a pair of planes produce the same line, then

$$\{p_{01} : p_{02} : p_{03} : p_{23} : p_{31} : p_{12}\} \equiv c\{P_{23} : P_{31} : P_{12} : P_{01} : P_{02} : P_{03}\}$$

where c is a non-zero real multiplier.

Now the condition that a point $B\{b_0 : b_1 : b_2 : b_3\}$ is on a line $p_a\{P_{01} : P_{02} : P_{03} : P_{23} : P_{31} : P_{12}\}$ is given as

$$X_i = \sum_{j=0}^{3} P_{ij}b_j = 0, (i = 0, 1, 2, 3) \tag{2.7}$$

where plane $x\{X_0 : X_1 : X_2 : X_3\}$ is expressed by a point B and a line p_a such that plane x vanishes.

CHAPTER 3

Architecture Synthesis of TPM Legs

In this chapter, a total of 90 leg architectures for three-legged symmetrical TPM are derived. Based on DGT, the procedure to synthesize TPM legs is simplified to a permutation and combination problem. Section 3.1 recalls all displacement subgroups and the kinematic bond $\{K_5(\mathbf{u}, \mathbf{v})\}$, which were introduced by Hervé (1978, 1999). Section 3.2 analyzes the characteristics of symmetrical TPMs, as well as some limitations in building TPM legs. The main synthesis procedure is dealt with in Section 3.3, where three categories of structures are classified.

3.1. Displacement Subgroups and Kinematic Bonds

3.1.1. Displacement Subgroups. As introduced in Section 2.2, a displacement forms a displacement subgroup if it meets the four conditions concurrently and if it is included in the displacement group $\{D\}$. The six lower kinematic pairs are regarded as six basic displacement subgroups as shown in Table 3.1, which was introduced in (Hervé, 1978). Note that N, $\mathbf{u}$, $\mathbf{v}$ and $\mathbf{w}$ denote a given orthogonal frame of reference, with N denoting the origin, vectors $\mathbf{u}$, $\mathbf{v}$ and $\mathbf{w}$ being three mutually orthogonal axes, and p standing for the pitch of a screw pair.

There are six other displacement subgroups which are not provided by any basic kinematic joint. These are shown in Table 3.2, which was introduced in (Hervé,

1978). Together with the first six, these twelve comprise all rigid-body displacement subgroups.

TABLE 3.1. Six basic subgroups of lower kinematic pairs.

Group of displacements	Dimension	Associated kinematic pairs
$\{R(N,\mathbf{u})\}$	1	Revolute pair R
$\{T(\mathbf{v})\}$	1	Prismatic pair P
$\{H(N,\mathbf{u},p)\}$	1	Screw pair H
$\{C(N,\mathbf{v})\}$	2	Cylindrical pair C
$\{G(\mathbf{u})\}$	3	Planar pair G
$\{S(N)\}$	3	Spherical pair S

TABLE 3.2. Six other subgroups of rigid-body displacements.

Group of displacements	Dimension	Name or typical motion
$\{I\}$	0	Identity subgroup
$\{T_2(\mathbf{u},\mathbf{v})\}$	2	Planar translational subgroup
$\{T_3(\mathbf{u},\mathbf{v},\mathbf{w}\}$	3	Spatial translational subgroup
$\{Y(\mathbf{u},p)\}$	3	Translating-screw subgroup
$\{X(\mathbf{w})\}$	4	Schönflies subgroup
$\{D\}$	6	Displacement group

Note that in Table 3.2, the translating-screw subgroup $\{Y(\mathbf{u}, p)\}$ allows a screw motion with axial direction $\mathbf{u}$, combined with two translational motions whose directions are normal to the vector $\mathbf{u}$; the Schönflies subgroup $\{X(\mathbf{w})\}$ allows three-direction translations and one rotation about the vector $\mathbf{w}$. Finally $\{D\}$ is the entire displacement group itself.

Now based on the above twelve displacement subgroups, a combination of some may be used to synthesize mechanisms capable of some desired, special spatial motions having fewer than six dofs.

3.1.2. Kinematic Bond. Combining a certain number of displacement subgroups to yield a serial kinematic chain, capable of producing a constrained relative motion, generates a kinematic bond. A kinematic bond itself can be a subgroup. For example, a combination of two translational subgroups $\{T(\mathbf{u})\}$ and $\{T(\mathbf{v})\}$, where vectors $\mathbf{u}$ and $\mathbf{v}$ are not parallel, yields a $\{T_2(\mathbf{u}, \mathbf{v})\}$ subgroup. Moreover, a kinematic bond can also be a non-group. For example, a combination of a rotational subgroup $\{R(N, \mathbf{u})\}$ and a second rotational subgroup $\{R(N, \mathbf{v})\}$ is not a subgroup, if vector $\mathbf{u}$ is not parallel to vector $\mathbf{v}$.

For kinematic bonds, two operations are employed, the intersection "$\cap$" and the product "$\cdot$", to generate the desired motion. An intersection operation "$\cap$" between two or more kinematic bonds indicates motion common to each kinematic chain, and the specific motions peculiar to one chain but not shared by others are mutually counteracted. A product operation "$\cdot$" between two or more displacement subgroups is the overall effect of different groups, so that the motion produced by the kinematic bond includes all the motions of each subgroup element.

Examples are given in the following two equations to illustrate the two operations.

$$\{T(\mathbf{u})\} \cdot \{R(\mathbf{u})\} \cdot \{R(\mathbf{u})\} \cdot \{R(\mathbf{u})\} = \{X(\mathbf{u})\} \tag{3.1}$$

Equation (3.1) indicates that the product of four subgroups, in the sequence of one translational subgroup and three rotational subgroups as shown above, yields the Schönflies subgroup.

$$\{X(\mathbf{z}_1)\} \cap \{X(\mathbf{z}_2)\} \cap \{X(\mathbf{z}_3)\} = \{T_3(\mathbf{u}, \mathbf{v}, \mathbf{w})\} \tag{3.2}$$

Equation (3.2) indicates that the intersection of three Schönflies subgroups yields the spatial translational subgroup, capable of spatial translations. The definitions of the symbols employed here are specified in Tables 3.1 and 3.2. Actually, the

combination displayed by Eq. (3.2) exactly represents the mechanical structure of Clavel's Delta robot (1988), where each leg provides the motion of a Schönflies subgroup. Note that for the Delta robot, the three vectors of three Schönflies subgroups $\{X(\mathbf{z}_i)\}$ $(i = 1, 2, 3)$ are coplanar, meaning that vectors $\mathbf{z}_1$, $\mathbf{z}_2$ and $\mathbf{z}_3$ are in the plane defined by vectors $\mathbf{u}$ and $\mathbf{v}$. Therefore, they are all perpendicular to vector $\mathbf{w}$.

Now a specific kinematic bond, called $\{K_5(\mathbf{u}, \mathbf{v})\}$, is recalled as having five dofs, three translations in three-dimensional space and two rotations not parallel to the one about the vector $\mathbf{w}$, which is defined to be perpendicular to vectors $\mathbf{u}$ and $\mathbf{v}$ simultaneously. Kinematic bond $\{K_5(\mathbf{u}, \mathbf{v})\}$ presents the third possibility for a symmetrical TPM leg, and will be employed in the following Section.

3.2. General Analysis of TPM Architectures

As mentioned in Section 3.1, the motion common to legs of a TPM is that of the moving platform. Therefore, the main task in TPM type synthesis is to design the leg architectures to be combined to form the entire parallel manipulator desired. Each leg is a serial kinematic chain containing a set of joints. The chain can be constructed using the six lower kinematic pairs, listed in Table 3.1, as basic synthesis elements.

Note that this thesis is devoted to the synthesis of three-legged TPMs. Since the EE has three dofs, three actuators, one for each leg, are appropriate and sufficient to drive the moving platform. Also, this architecture accounts for most existing TPMs. Architectural complications, such as doubly actuated and redundant legs, make non three-legged TPMs much less popular. Therefore, they are not considered here.

Now, with the intention to generate translational motion of the moving platform, the three categories defined below provide three basic rules to synthesize TPMs with symmetrical base and platform and three identical legs. These three categories describe all possible cases in the synthesis procedure.

Category 1:

$$\{T_3(\mathbf{u}, \mathbf{v}, \mathbf{w})\} \cap \{T_3(\mathbf{u}, \mathbf{v}, \mathbf{w})\} \cap \{T_3(\mathbf{u}, \mathbf{v}, \mathbf{w})\} = \{T_3(\mathbf{u}, \mathbf{v}, \mathbf{w})\} \tag{3.3}$$

Category 2:

$$\{X(\mathbf{w}_1)\} \cap \{X(\mathbf{w}_2)\} \cap \{X(\mathbf{w}_3)\} = \{T_3(\mathbf{u}, \mathbf{v}, \mathbf{w})\} \tag{3.4}$$

Category 3:

$$\{K_5(\mathbf{u}_1, \mathbf{v}_1)\} \cap \{K_5(\mathbf{u}_2, \mathbf{v}_2)\} \cap \{K_5(\mathbf{u}_3, \mathbf{v}_3)\} = \{T_3(\mathbf{u}, \mathbf{v}, \mathbf{w})\} \tag{3.5}$$

Equation (3.3) means that a combination of three spatial translational subgroups is still the same, which is obvious. Equation (3.4) shows that a combination of three Schönflies subgroups forms the spatial translational subgroup, a typical example of which is the well-known Delta robot. For Eq. (3.5), $\{K_5(\mathbf{u}_1, \mathbf{v}_1)\}$ is defined in Section 3.1 and the entire equation means that a combination of three kinematic bonds $\{K_5(\mathbf{u}_1, \mathbf{v}_1)\}$ also produces the $\{T_3(\mathbf{u}, \mathbf{v}, \mathbf{w})\}$ subgroup. For the second and third cases, the conflicting rotational dofs are cancelled among legs. The key point here is that each leg should have at least three translational dofs, but less than six, including the three rotations, in three-dimensional space. Hence, it is implied that spherical joints cannot be employed in symmetrical TPM design because of their three rotational dofs. Moreover, any revolute, screw or cylindrical joint that rotates about an axis parallel to the vector $\mathbf{w}$, which is perpendicular to vectors $\mathbf{u}$ and $\mathbf{v}$, should be avoided. Furthermore, if a planar subgroup $\{G(\mathbf{u})\}$ is employed in the synthesis, one should notice that the vectors $\mathbf{u}$ and $\mathbf{w}$ should not be parallel.

For TPMs with asymmetrical architectures, the two subgroups $\{T_3(\mathbf{u}, \mathbf{v}, \mathbf{w})\}$ and $\{X(\mathbf{w}_1)\}$, and kinematic bond $\{K_5(\mathbf{u}_1, \mathbf{v}_1)\}$ remain the synthesis elements. An asymmetrical TPM can be generated by combining any three of them. Moreover, the entire displacement group $\{D\}$ may be used to synthesize an asymmetrical TPM in some cases as well. However, commonly preferred TPM architectures with topologically identical leg geometry require fewer kinds of components. Symmetrical TPMs are simpler and less expensive to manufacture, and hence avoid the loss of precision introduced by additional joints. This advantage is an important consideration in choosing a mechanism. Most existing industrial TPMs are symmetrical. Therefore, asymmetrical TPM architectures will not be delved into deeply.

3.3. Architecture Synthesis of TPM Legs

3.3.1. Category 1: $\boldsymbol{T}_3(\mathbf{u}, \mathbf{v}, \mathbf{w})$ Subgroup. The synthesis based on this subgroup is elementary. Since each leg of the mechanism admits translational motion without rotation, only prismatic joints apply. As each leg contains only translational joints, the rotation of the moving platform is impossible. The three legs have no internal constraining relations like the Delta robot that involves cancellation of conflicting rotational dof. Therefore, any leg synthesized from the spatial translational subgroup can perform the desired motion individually; and actually, such an architecture is overconstrained, because any constraint is repeated three times. A leg architecture schematic is shown in Fig. 3.1.

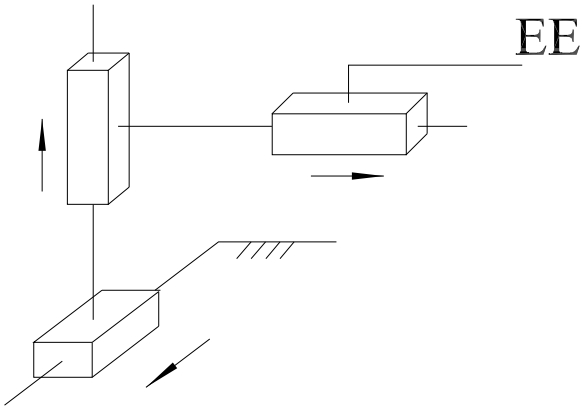

FIGURE 3.1. Leg architecture of spatial translational subgroup.

3.3.2. Category 2: $\{\boldsymbol{X}(\mathbf{w}_1)\}$ Schönflies Subgroup. The Schönflies subgroup is a Schönflies-motion generator, allowing three translations and one rotation. Obviously, the three translational dofs can be represented by a three-dimensional spatial translational subgroup, namely $\{T_3(\mathbf{u}_1, \mathbf{v}_1, \mathbf{w}_1)\}$, while the one-dof rotation can be represented by a rotational subgroup $\{R(\mathbf{w}_1)\}$. Therefore, the algebraic expression for legs of the Schönflies subgroup architecture is shown as

$$\{X(\mathbf{w}_1)\} = \{T_3(\mathbf{u}_1, \mathbf{v}_1, \mathbf{w}_1)\} \cdot \{R(\mathbf{w}_1)\} \tag{3.6}$$

However, Eq. (3.6) displays a trivial case of TPM leg synthesis, because the spatial translational subgroup $\{T_3(\mathbf{u}_1, \mathbf{v}_1, \mathbf{w}_1)\}$ has already fulfilled the aim of translations in three-dimensional space. Hence, the rotational subgroup added to each leg is useless and irrelevant as regards realization of spatial translations.

An alternative implementation of the Schönflies subgroup $\{X(\mathbf{w}_1)\}$ is given, indicating that the Schönflies motion can be generated by combining a planar subgroup and a translational subgroup.

$$\{X(\mathbf{w}_1)\} = \{G(\mathbf{w}_1)\} \cdot \{T(\mathbf{w}_1)\} \tag{3.7}$$

Table 3.3 displays the possible planar subgroup constitutions formed by combining rotational and translational subgroups.

TABLE 3.3. Kinematic bond and joint configuration for the planar subgroup.

	Kinematic bond	Joint configuration
$\{G(\mathbf{w}_1)\}$	$\{T(\mathbf{u}_1)\} \cdot \{T(\mathbf{v}_1)\} \cdot \{R(\mathbf{w}_1)\}$	P P R
	$\{T(\mathbf{u}_1)\} \cdot \{R(\mathbf{w}_1)\} \cdot \{T(\mathbf{v}_1)\}$	P R P
	$\{R(\mathbf{w}_1)\} \cdot \{T(\mathbf{u}_1)\} \cdot \{T(\mathbf{v}_1)\}$	R P P
	$\{R(\mathbf{w}_1)\} \cdot \{R(\mathbf{w}_1)\} \cdot \{T(\mathbf{u}_1)\}$	R R P
	$\{R(\mathbf{w}_1)\} \cdot \{T(\mathbf{u}_1)\} \cdot \{R(\mathbf{w}_1)\}$	R P R
	$\{T(\mathbf{u}_1)\} \cdot \{R(\mathbf{w}_1)\} \cdot \{R(\mathbf{w}_1)\}$	P R R
	$\{R(\mathbf{w}_1)\} \cdot \{R(\mathbf{w}_1)\} \cdot \{R(\mathbf{w}_1)\}$	R R R

Note that vectors $\mathbf{u}_1$, $\mathbf{v}_1$ and $\mathbf{w}_1$ differ from vectors $\mathbf{u}$, $\mathbf{v}$ and $\mathbf{w}$ in Tables 3.1 and 3.2 in that the former need not be mutually orthogonal. Now together with the translational subgroup in Eq. (3.7) and removing repeated ones, a total of 14 possible leg architectures are obtained. Their configurations are shown in Table 3.4.

Class 1 in Table 3.4 is the the same as the one synthesized with Eq. (3.6) except for a shuffle of the revolute joint position. That is because the Schönflies subgroup can be divided either into a combination of a spatial translational subgroup and a

TABLE 3.4. All possible leg architectures for the Schönflies subgroup.

Classification	Kinematic bond
Class 1: Three $\{T\}$ subgroups	$\{T(\mathbf{w}_1)\} \cdot \{T(\mathbf{u}_1)\} \cdot \{T(\mathbf{v}_1)\} \cdot \{R(\mathbf{w}_1)\}$
	$\{T(\mathbf{w}_1)\} \cdot \{T(\mathbf{u}_1)\} \cdot \{R(\mathbf{w}_1)\} \cdot \{T(\mathbf{v}_1)\}$
	$\{T(\mathbf{w}_1)\} \cdot \{R(\mathbf{w}_1)\} \cdot \{T(\mathbf{u}_1)\} \cdot \{T(\mathbf{v}_1)\}$
	$\{R(\mathbf{w}_1)\} \cdot \{T(\mathbf{w}_1)\} \cdot \{T(\mathbf{u}_1)\} \cdot \{T(\mathbf{v}_1)\}$
Class 2: Two $\{T\}$ subgroups	$\{T(\mathbf{w}_1)\} \cdot \{R(\mathbf{w}_1)\} \cdot \{R(\mathbf{w}_1)\} \cdot \{T(\mathbf{u}_1)\}$
	$\{R(\mathbf{w}_1)\} \cdot \{T(\mathbf{w}_1)\} \cdot \{R(\mathbf{w}_1)\} \cdot \{T(\mathbf{u}_1)\}$
	$\{R(\mathbf{w}_1)\} \cdot \{R(\mathbf{w}_1)\} \cdot \{T(\mathbf{w}_1)\} \cdot \{T(\mathbf{u}_1)\}$
	$\{T(\mathbf{w}_1)\} \cdot \{R(\mathbf{w}_1)\} \cdot \{T(\mathbf{u}_1)\} \cdot \{R(\mathbf{w}_1)\}$
	$\{R(\mathbf{w}_1)\} \cdot \{T(\mathbf{w}_1)\} \cdot \{T(\mathbf{u}_1)\} \cdot \{R(\mathbf{w}_1)\}$
	$\{T(\mathbf{w}_1)\} \cdot \{T(\mathbf{u}_1)\} \cdot \{R(\mathbf{w}_1)\} \cdot \{R(\mathbf{w}_1)\}$
Class 3: One $\{T\}$ subgroup	$\{T(\mathbf{w}_1)\} \cdot \{R(\mathbf{w}_1)\} \cdot \{R(\mathbf{w}_1)\} \cdot \{R(\mathbf{w}_1)\}$
	$\{R(\mathbf{w}_1)\} \cdot \{T(\mathbf{w}_1)\} \cdot \{R(\mathbf{w}_1)\} \cdot \{R(\mathbf{w}_1)\}$
	$\{R(\mathbf{w}_1)\} \cdot \{R(\mathbf{w}_1)\} \cdot \{T(\mathbf{w}_1)\} \cdot \{R(\mathbf{w}_1)\}$
	$\{R(\mathbf{w}_1)\} \cdot \{R(\mathbf{w}_1)\} \cdot \{R(\mathbf{w}_1)\} \cdot \{T(\mathbf{w}_1)\}$

rotational subgroup, or into a combination of a planar subgroup and a translational subgroup. Therefore, Eqs. (3.6) and (3.7) are equivalent. But Eq. (3.7) conveys more details than Eq. (3.6). As previously mentioned, three translational subgroups meet the synthesis requirement. Hence, the first class is ignored. Figures 3.2 and 3.3 show synthesized architecture schematics for classes 2 and 3.

3.3.3. Category 3: Kinematic Bond $\{\boldsymbol{K}_5(\mathbf{u}_1, \mathbf{v}_1)\}$. Leg architectures with five dofs constitute kinematic bonds but not subgroups because they do not satisfy all group properties. The five-dof kinematic bond mentioned here includes three-direction translations and two rotations different from the one about the normal to the horizontal plane, assuming that the base plane is considered horizontal. Again,

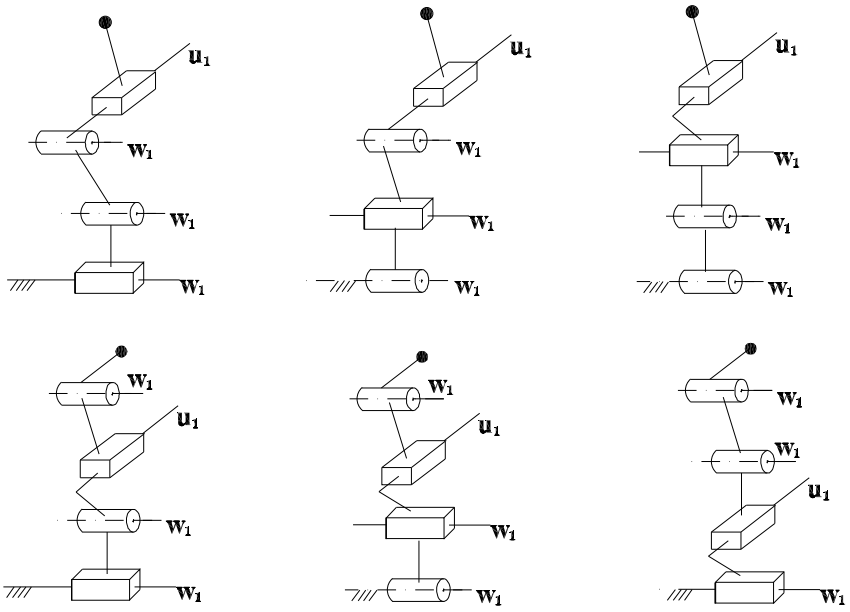

FIGURE 3.2. Leg architectures of class 2.

in this case, the two rotational dofs for each leg are mutually counteracted and only translations in three-dimensional space are preserved for the EE motion.

Based on the kinematic characteristics of the kinematic bond $\{K_5(\mathbf{u}_1, \mathbf{v}_1)\}$, apparently, it can be formed by combining one spatial translational subgroup and two rotational subgroups.

$$\{K_5(\mathbf{u}_1, \mathbf{v}_1)\} = \{T_3(\mathbf{u}_1, \mathbf{v}_1, \mathbf{w}_1)\} \cdot \{R(\mathbf{u}_1)\} \cdot \{R(\mathbf{v}_1)\} \tag{3.8}$$

However, the same problem occurs again as with Eq. (3.6) where the three-dimensional translations provided by subgroup $\{T_3(\mathbf{u}_1, \mathbf{v}_1, \mathbf{w}_1)\}$ renders the two rotational subgroups useless. Therefore, Eq. (3.8) cannot be regarded as a synthesis formula. A more general alternative expression is given herein.

$$\{K_5(\mathbf{u}_1, \mathbf{v}_1)\} = \{G(\mathbf{u}_1)\} \cdot \{G(\mathbf{v}_1)\} \tag{3.9}$$

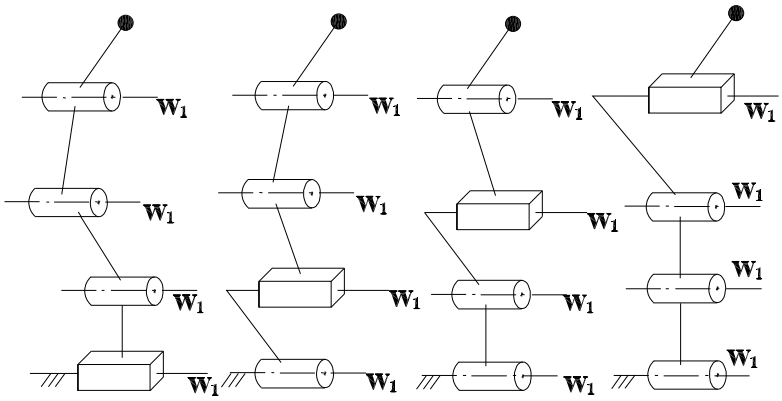

FIGURE 3.3. Leg architectures of class 3.

In Eq. (3.9), the kinematic bond $\{K_5(\mathbf{u}_1, \mathbf{v}_1)\}$ is divided into two planar subgroups, whose axes of rotation $\mathbf{u}_1$ and $\mathbf{v}_1$ are not parallel. Although one planar subgroup has three dofs, a combination of two does not give six because they share one common translation which is in the direction of the normal to the plane defined by vectors $\mathbf{u}_1$ and $\mathbf{v}_1$ as shown in Fig. 3.4.

Now we recall Table 3.3. It is clear that this table presents in general three cases for the constitution of a planar subgroup.

$$\{G(\mathbf{w}_1)\} = \{T(\mathbf{u}_1)\} \cdot \{T(\mathbf{v}_1)\} \cdot \{R(\mathbf{w}_1)\} \tag{3.10}$$

$$\{G(\mathbf{w}_1)\} = \{R(\mathbf{w}_1)\} \cdot \{R(\mathbf{w}_1)\} \cdot \{T(\mathbf{u}_1)\} \tag{3.11}$$

$$\{G(\mathbf{w}_1)\} = \{R(\mathbf{w}_1)\} \cdot \{R(\mathbf{w}_1)\} \cdot \{R(\mathbf{w}_1)\} \tag{3.12}$$

Choosing any two of these three equations to substitute into Eq. (3.9) produces an equation from which a kinematic bond $\{K_5(\mathbf{u}_1, \mathbf{v}_1)\}$ can be synthesized. However, if two of Eq. (3.10) are selected, there will be four translational subgroups, which is impractical since three-dimensional space only allows three translations. Hence, such a situation is omitted. Besides, a combination of Eqs. (3.10) and (3.12) is equivalent

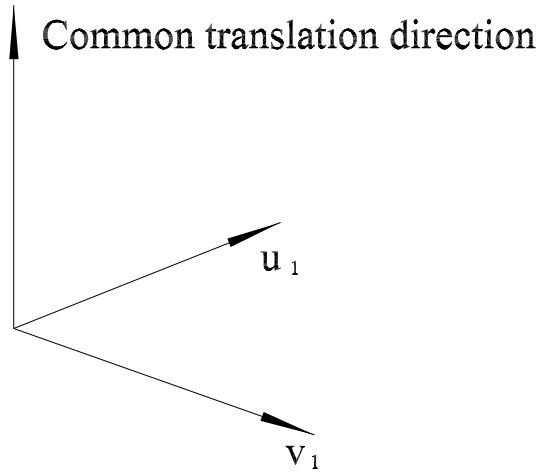

FIGURE 3.4. Common translation perpendicular to vectors $\mathbf{u}_1$ and $\mathbf{v}_1$.

to a combination of twice Eq. (3.11), hence another case may be removed. Therefore, four possible situations remain, namely the following four equations where repeated subgroups have been omitted. Note that the unit vectors $\mathbf{u}_1$, $\mathbf{v}_1$ and $\mathbf{w}_1$ are defined in such a way that vector $\mathbf{w}_1$ is in the direction of $\mathbf{u}_1 \times \mathbf{v}_1$. The vector $\mathbf{w}_1$ can be normal to the horizontal plane.

$$\{K_5(\mathbf{u}_1, \mathbf{v}_1)\} = \{T(\mathbf{w}_1)\} \cdot \{T(\mathbf{v}_1)\} \cdot \{R(\mathbf{u}_1)\} \cdot \{T(\mathbf{u}_1)\} \cdot \{R(\mathbf{v}_1)\} \tag{3.13}$$

$$\{K_5(\mathbf{u}_1, \mathbf{v}_1)\} = \{R(\mathbf{u}_1)\} \cdot \{R(\mathbf{u}_1)\} \cdot \{T(\mathbf{w}_1)\} \cdot \{R(\mathbf{v}_1)\} \cdot \{T(\mathbf{u}_1)\} \tag{3.14}$$

$$\{K_5(\mathbf{u}_1, \mathbf{v}_1)\} = \{R(\mathbf{u}_1)\} \cdot \{R(\mathbf{u}_1)\} \cdot \{R(\mathbf{v}_1)\} \cdot \{R(\mathbf{v}_1)\} \cdot \{T(\mathbf{w}_1)\} \tag{3.15}$$

$$\{K_5(\mathbf{u}_1, \mathbf{v}_1)\} = \{R(\mathbf{u}_1)\} \cdot \{R(\mathbf{u}_1)\} \cdot \{R(\mathbf{u}_1)\} \cdot \{R(\mathbf{v}_1)\} \cdot \{R(\mathbf{v}_1)\} \tag{3.16}$$

Based on each synthesis equation, the corresponding leg architectures are shown in Tables 3.5 through 3.8.

The architectures listed in Table 3.5 are similar to class 1 of Subsection 3.3.2 in that each leg has three translational subgroups, which are sufficient to perform

TABLE 3.5. Kinematic bond $\{K_5(\mathbf{u}_1, \mathbf{v}_1)\}$ with three translational subgroups.

Class 4: Three $\{T\}$ subgroups	$\{T(\mathbf{w}_1)\} \cdot \{T(\mathbf{u}_1)\} \cdot \{T(\mathbf{v}_1)\} \cdot \{R(\mathbf{u}_1)\} \cdot \{R(\mathbf{v}_1)\}$
	$\{R(\mathbf{u}_1)\} \cdot \{T(\mathbf{w}_1)\} \cdot \{T(\mathbf{u}_1)\} \cdot \{T(\mathbf{v}_1)\} \cdot \{R(\mathbf{v}_1)\}$
	$\{R(\mathbf{u}_1)\} \cdot \{R(\mathbf{v}_1)\} \cdot \{T(\mathbf{w}_1)\} \cdot \{T(\mathbf{u}_1)\} \cdot \{T(\mathbf{v}_1)\}$
	$\{T(\mathbf{w}_1)\} \cdot \{R(\mathbf{u}_1)\} \cdot \{R(\mathbf{v}_1)\} \cdot \{T(\mathbf{u}_1)\} \cdot \{T(\mathbf{v}_1)\}$
	$\{T(\mathbf{w}_1)\} \cdot \{T(\mathbf{u}_1)\} \cdot \{R(\mathbf{u}_1)\} \cdot \{R(\mathbf{v}_1)\} \cdot \{T(\mathbf{v}_1)\}$
	$\{T(\mathbf{w}_1)\} \cdot \{R(\mathbf{u}_1)\} \cdot \{T(\mathbf{u}_1)\} \cdot \{T(\mathbf{v}_1)\} \cdot \{R(\mathbf{v}_1)\}$
	$\{T(\mathbf{u}_1)\} \cdot \{T(\mathbf{v}_1)\} \cdot \{R(\mathbf{u}_1)\} \cdot \{T(\mathbf{w}_1)\} \cdot \{R(\mathbf{v}_1)\}$
	$\{R(\mathbf{u}_1)\} \cdot \{T(\mathbf{w}_1)\} \cdot \{R(\mathbf{v}_1)\} \cdot \{T(\mathbf{u}_1)\} \cdot \{T(\mathbf{v}_1)\}$
	$\{R(\mathbf{u}_1)\} \cdot \{T(\mathbf{w}_1)\} \cdot \{T(\mathbf{u}_1)\} \cdot \{R(\mathbf{v}_1)\} \cdot \{T(\mathbf{v}_1)\}$
	$\{T(\mathbf{w}_1)\} \cdot \{R(\mathbf{u}_1)\} \cdot \{T(\mathbf{u}_1)\} \cdot \{R(\mathbf{v}_1)\} \cdot \{T(\mathbf{v}_1)\}$

three-dimensional translations. Therefore, the revolute joints in class 4 are inactive and do not contribute to the motion generation of spatial translations.

There are a total of 30 cases for the kinematic bond $\{K_5(\mathbf{u}_1, \mathbf{v}_1)\}$ with two translational subgroups, and based theoretically on Eq. (3.14). Since there are three rotational subgroups and two translational subgroups, arranging their order is only a permutation and combination problem. In Table 3.6, three possible architectures are described, with 27 remaining cases omitted to keep the tabulation concise. For each architecture shown in Table 3.6, the order of the three rotational subgroups is different; there are in all 10 possible combinations for each of the three cases. That is, each kinematic bond listed there can be considered as a generator of 10 leg architectures in this class.

The kinematic bond $\{K_5(\mathbf{u}_1, \mathbf{v}_1)\}$, with one translational subgroup, is a more complicated case. There are two ways to choose the four rotational subgroups. For instance, one can choose three identical ones and one different, meaning that the axes of three revolute joints are parallel, while one is not. Alternatively, one can choose a pair of different identical pairs. The first case is again a permutation and combination

TABLE 3.6. Kinematic bond $\{K_5(\mathbf{u}_1, \mathbf{v}_1)\}$ with two translational subgroups.

Class 5: Two $\{T\}$ subgroups	$\{R(\mathbf{u}_1)\} \cdot \{R(\mathbf{u}_1)\} \cdot \{R(\mathbf{v}_1)\} \cdot \{T(\mathbf{w}_1)\} \cdot \{T(\mathbf{u}_1)\}$
	$\{R(\mathbf{u}_1)\} \cdot \{R(\mathbf{v}_1)\} \cdot \{R(\mathbf{u}_1)\} \cdot \{T(\mathbf{w}_1)\} \cdot \{T(\mathbf{u}_1)\}$
	$\{R(\mathbf{v}_1)\} \cdot \{R(\mathbf{u}_1)\} \cdot \{R(\mathbf{u}_1)\} \cdot \{T(\mathbf{w}_1)\} \cdot \{T(\mathbf{u}_1)\}$

problem. All one needs to do is to vary the position of the prismatic joint with respect to the four revolute joints. There are four possible arrangements for the four revolute joints as follows:

$$\{R(\mathbf{u}_1)\} \cdot \{R(\mathbf{u}_1)\} \cdot \{R(\mathbf{u}_1)\} \cdot \{R(\mathbf{v}_1)\} \tag{3.17}$$

$$\{R(\mathbf{u}_1)\} \cdot \{R(\mathbf{u}_1)\} \cdot \{R(\mathbf{v}_1)\} \cdot \{R(\mathbf{u}_1)\} \tag{3.18}$$

$$\{R(\mathbf{u}_1)\} \cdot \{R(\mathbf{v}_1)\} \cdot \{R(\mathbf{u}_1)\} \cdot \{R(\mathbf{u}_1)\} \tag{3.19}$$

$$\{R(\mathbf{v}_1)\} \cdot \{R(\mathbf{u}_1)\} \cdot \{R(\mathbf{u}_1)\} \cdot \{R(\mathbf{u}_1)\} \tag{3.20}$$

For each arrangement, there are five possible prismatic joint sites. Therefore, for the first case, three identical rotational subgroups and a differing fourth, there are 20 possible architectures.

For the second case, the sequence of the four rotational subgroups cannot be arbitrary. As Carricato and Parenti-Castelli (2002) state, at least two identically oriented revolute joints should be kept adjacent; therefore, there are two possible arrangements of revolute joints as shown below. The prismatic joint placement remains arbitrary.

$$\{R(\mathbf{u}_1)\} \cdot \{R(\mathbf{u}_1)\} \cdot \{R(\mathbf{v}_1)\} \cdot \{R(\mathbf{v}_1)\} \tag{3.21}$$

$$\{R(\mathbf{u}_1)\} \cdot \{R(\mathbf{v}_1)\} \cdot \{R(\mathbf{v}_1)\} \cdot \{R(\mathbf{u}_1)\} \tag{3.22}$$

To summarize cases represented by Eqs. (3.17) through (3.22), Table 3.7 shows six possible leg architectures for the kinematic bond $\{K_5(\mathbf{u}_1, \mathbf{v}_1)\}$ with one translational subgroup. Similar to Table 3.6, each listed configuration implies four other possibilities.

TABLE 3.7. Kinematic bond $\{K_5(\mathbf{u}_1, \mathbf{v}_1)\}$ with one translational subgroup.

Class 6: One $\{T\}$ subgroup	$\{R(\mathbf{u}_1)\} \cdot \{R(\mathbf{u}_1)\} \cdot \{R(\mathbf{u}_1)\} \cdot \{R(\mathbf{v}_1)\} \cdot \{T(\mathbf{w}_1)\}$
	$\{R(\mathbf{u}_1)\} \cdot \{R(\mathbf{u}_1)\} \cdot \{R(\mathbf{v}_1)\} \cdot \{R(\mathbf{u}_1)\} \cdot \{T(\mathbf{w}_1)\}$
	$\{R(\mathbf{u}_1)\} \cdot \{R(\mathbf{v}_1)\} \cdot \{R(\mathbf{u}_1)\} \cdot \{R(\mathbf{u}_1)\} \cdot \{T(\mathbf{w}_1)\}$
	$\{R(\mathbf{v}_1)\} \cdot \{R(\mathbf{u}_1)\} \cdot \{R(\mathbf{u}_1)\} \cdot \{R(\mathbf{u}_1)\} \cdot \{T(\mathbf{w}_1)\}$
	$\{R(\mathbf{u}_1)\} \cdot \{R(\mathbf{u}_1)\} \cdot \{R(\mathbf{v}_1)\} \cdot \{R(\mathbf{v}_1)\} \cdot \{T(\mathbf{w}_1)\}$
	$\{R(\mathbf{u}_1)\} \cdot \{R(\mathbf{v}_1)\} \cdot \{R(\mathbf{v}_1)\} \cdot \{R(\mathbf{u}_1)\} \cdot \{T(\mathbf{w}_1)\}$

For the situation described in Eq. (3.16), containing no translational subgroup, there are three parallel revolute joints and two in another direction but mutually parallel. Theoretically, there are 10 possible leg architectures. However, at least one parallel pair must remain adjacent. Therefore, five out of ten are thus eliminated and the remaining five are listed in Table 3.8.

TABLE 3.8. Kinematic bond $\{K_5(\mathbf{u}_1, \mathbf{v}_1)\}$ with no translational subgroup.

Class 7: No $\{T\}$ subgroup	$\{R(\mathbf{u}_1)\} \cdot \{R(\mathbf{u}_1)\} \cdot \{R(\mathbf{u}_1)\} \cdot \{R(\mathbf{v}_1)\} \cdot \{R(\mathbf{v}_1)\}$
	$\{R(\mathbf{u}_1)\} \cdot \{R(\mathbf{v}_1)\} \cdot \{R(\mathbf{v}_1)\} \cdot \{R(\mathbf{u}_1)\} \cdot \{R(\mathbf{u}_1)\}$
	$\{R(\mathbf{u}_1)\} \cdot \{R(\mathbf{u}_1)\} \cdot \{R(\mathbf{v}_1)\} \cdot \{R(\mathbf{v}_1)\} \cdot \{R(\mathbf{u}_1)\}$
	$\{R(\mathbf{v}_1)\} \cdot \{R(\mathbf{v}_1)\} \cdot \{R(\mathbf{u}_1)\} \cdot \{R(\mathbf{u}_1)\} \cdot \{R(\mathbf{u}_1)\}$
	$\{R(\mathbf{v}_1)\} \cdot \{R(\mathbf{u}_1)\} \cdot \{R(\mathbf{u}_1)\} \cdot \{R(\mathbf{u}_1)\} \cdot \{R(\mathbf{v}_1)\}$

Four representatives of classes 4 through 7 are shown in Fig. 3.5 to indicate leg architectures that constitute kinematic bond $\{K_5(\mathbf{u}_1, \mathbf{v}_1)\}$.

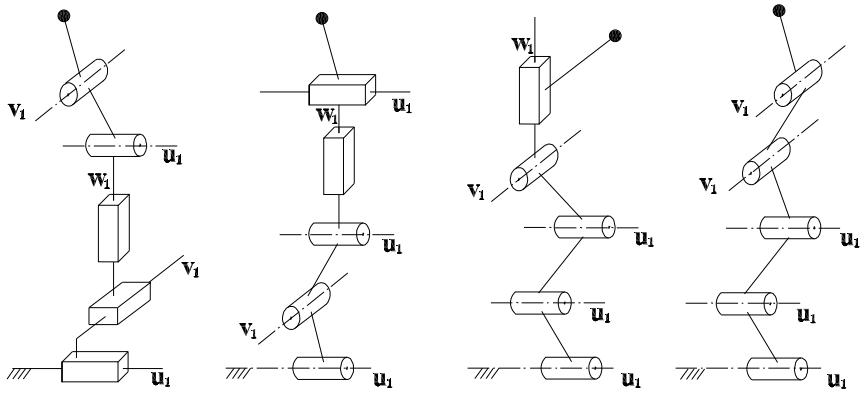

FIGURE 3.5. Several leg architectures for classes 4-7.

So far, the whole class of 90 leg architectures for three-legged symmetrical TPMs has been synthesized.

CHAPTER 4

Type Synthesis of TPMs

In this chapter, TPM types, including both symmetrical and asymmetrical ones, are synthesized. Section 4.1 introduces joint replacements. Section 4.2 presents the symmetrical TPMs, as well as some TPM variations. Section 4.3 presents type synthesis of asymmetrical TPMs. A comparison of different synthesis methods and the advantages of DGT are discussed in Section 4.4.

4.1. Joint Replacements for Leg Architectures

For the leg architectures of categories 2 and 3 mentioned in Sections 3.2 and 3.3, only the translational subgroup and rotational subgroup are employed. When considering other subgroups, such as the cylindrical subgroup, and joint replacements, one can obtain a more comprehensive set of leg architectures.

It is well known that a cylindrical joint can be used to replace an adjacent prismatic and revolute joint, provided that the revolute axis is parallel to the translation direction of the prismatic joint. Moreover, a four-bar parallelogram, called the Π joint, comprising four revolute joints with parallel axes and four links in parallelogram array, can be used to generate the third type of translation wherein points move on circular paths. Therefore, one can synthesize additional leg architectures of category 2 with the cylindrical joint and the four-bar parallelogram. Figure 4.1 shows these two architectures.

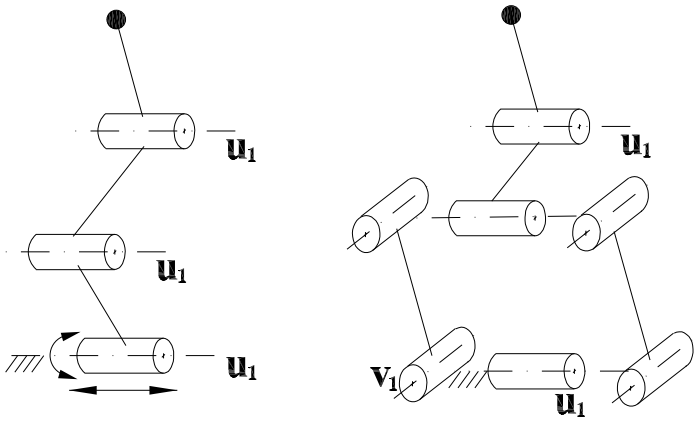

FIGURE 4.1. Leg architectures with cylindrical joint and parallelogram.

Besides the two substitutions mentioned above, two adjacent revolute joints with nonparallel axes can be replaced by a universal joint. Different category 3 architectures can also be obtained as shown in Fig. 4.2.

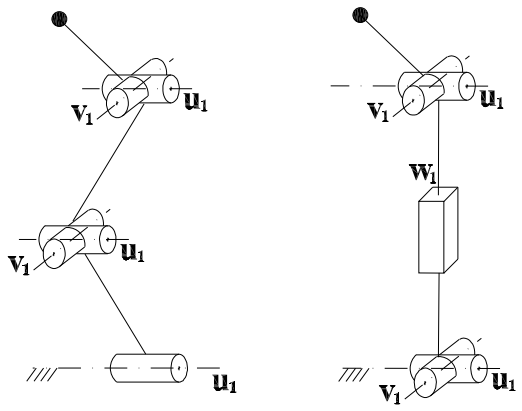

FIGURE 4.2. Leg architectures with universal joints.

With the above-mentioned joint replacements, many different TPM structures can be obtained. Several practical examples will be given in the following section.

4.2. Type Synthesis of Symmetrical TPMs

Based on the leg architectures enumerated in Chapter 3, one can perform type synthesis of symmetrical TPMs by combining any three identical legs, with a base and moving platform. A generic TPM is shown in Fig. 4.3, where the kinematic chains between the base and the moving platform represent three identical legs.

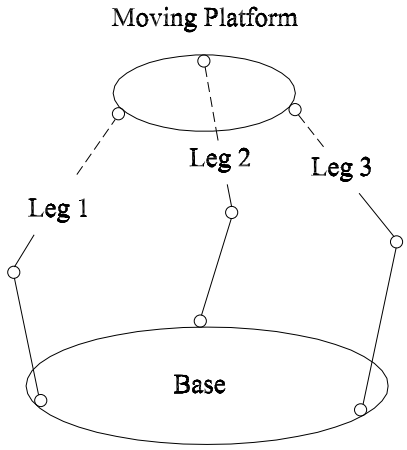

FIGURE 4.3. Prototype of a three-legged TPM.

We recall that, for leg architectures of classes 1 and 4, there are three translational subgroups in each leg to provide three-dimensional translation. The revolute joints are useless if the desired motion is confined to spatial translation. This was noted in Section 3.3 regarding TPM leg synthesis. However, when considering the entire TPM and selection of actuated joints, one cannot neglect these architectures. One may choose to actuate such revolute joints to produce the desired translation. Therefore, for symmetrical TPMs, a total of 90 possible configurations have been enumerated so far.

Now with some TPM variations obtained with joint replacements, the entire family of symmetrical TPM architectures has been described. All known and existing TPMs are included. For example, Kim and Tsai's Cartesian Parallel Manipulator

(CPM) (2003), as shown in Fig. 4.4, belongs to the first case of class 3, and admits two actuation options, revolute and prismatic. CPM has a structure of $\{T(\mathbf{w}_1)\} \cdot \{R(\mathbf{w}_1)\} \cdot \{R(\mathbf{w}_1)\} \cdot \{R(\mathbf{w}_1)\}$ and employs the originally synthesized subgroups.

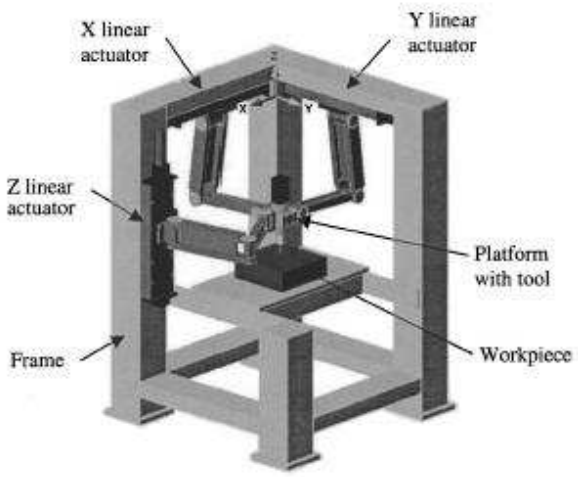

FIGURE 4.4. Kim and Tsai's CPM (2003).

Kong and Gosselin's $\underline{C}$RR manipulator (2002) is the outcome of replacing two adjacent prismatic and revolute joints with a cylindrical joint, as shown in Fig. 4.5. This manipulator has a structure of $\{T(\mathbf{w}_1)\} \cdot \{R(\mathbf{w}_1)\} \cdot \{R(\mathbf{w}_1)\} \cdot \{R(\mathbf{w}_1)\}$.

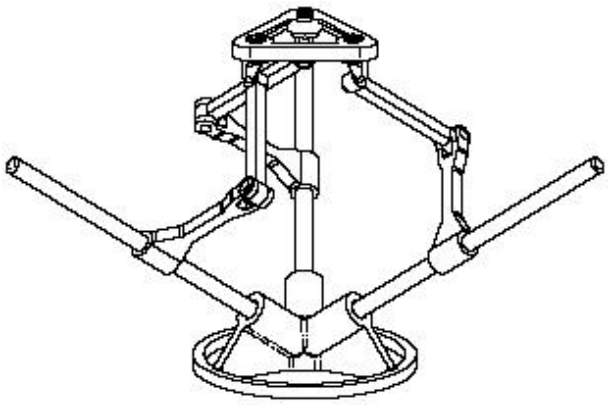

FIGURE 4.5. Kong and Gosselin's $\underline{C}$RR manipulator (2002).

Clavel's Delta robot (1988) is obtained by replacing the prismatic joint in class 3 with a four-bar parallelogram, as shown in Fig. 4.6. The leg architecture of Delta robot results from a subgroup product of $\{R(\mathbf{u}_1)\} \cdot \{R(\mathbf{u}_1)\} \cdot \{T(\mathbf{w}_1)\} \cdot \{R(\mathbf{u}_1)\}$.

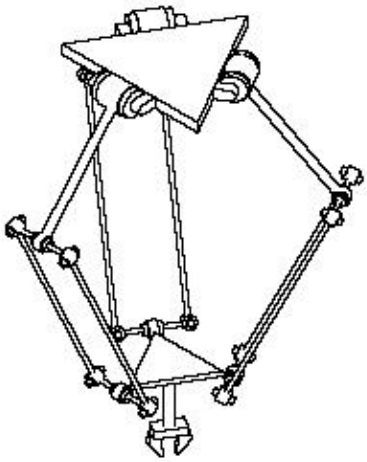

FIGURE 4.6. Clavel's Delta robot (1988).

The Orthoglide proposed by Chablat and Wenger (2003) is a variation of case 4 in class 2 by using the parallelogram instead of a prismatic joint. Fig. 4.7 shows its structure, which is a subgroup product of $\{T(\mathbf{w}_1)\} \cdot \{R(\mathbf{u}_1)\} \cdot \{T(\mathbf{u}_1)\} \cdot \{R(\mathbf{u}_1)\}$.

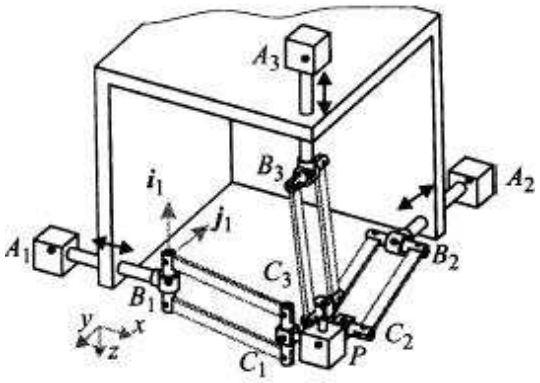

FIGURE 4.7. Chablat and Wenger's Orthoglide (2003).

4.3. Type Synthesis of Asymmetrical TPMs

For asymmetrical TPMs, displacement group $\{D\}$, which describes all the possible motions of a rigid body in three-dimensional space, can also be applied to construct a leg. Its rotational dof about the normal of the horizontal plane should be cancelled by the other two legs. For a six-dof kinematic chain, there is a great variety of architectures that may be synthesized. Therefore, six-dof leg architecture synthesis will not be investigated in this thesis.

In order to synthesize an asymmetrical TPM, there are four leg architectures to choose from, the three represented by Eqs. (3.3), (3.4) and (3.5), as well as the six-dof kinematic chain. Taking any three out of the four which are not all identical gives a maximum of sixteen possibilities; however, three of them are not applicable to TPM synthesis. By representing the corresponding dof of a kinematic chain with a number, for example, 3 represents the three-dof kinematic chain of category 1, the three omitted options are 4-6-6, 5-6-6 and 5-5-6, respectively. The remaining 13 constructions constitute asymmetrical TPM possibilities. This conclusion was reported by Kong and Gosselin (2004) as well.

Figure 4.8 shows some asymmetrical constructions. Selection is left to prospective designers. Because the asymmetrical structures rarely appear in practice, investigation of asymmetrical TPMs is discontinued herein.

4.4. A Comparison of Different Synthesis Methods

The previously reported synthesis methods for TPMs seem quite limited, even the most general one, based on screw theory, by Kong and Gosselin (2004). In their research, they utilized the screw concept to describe the legs. Thus the whole structure was represented by a system of constraining wrenches. By defining some conditions that a PKM has to satisfy in order to be a TPM, they obtained the whole class of TPMs with exhaustive constructions. The conclusion they draw is quite comprehensive, but, quite apart from screw theory, the synthesis argument is rather complicated. In a later paper, Kong and Gosselin (2004) employed the virtual joint, a

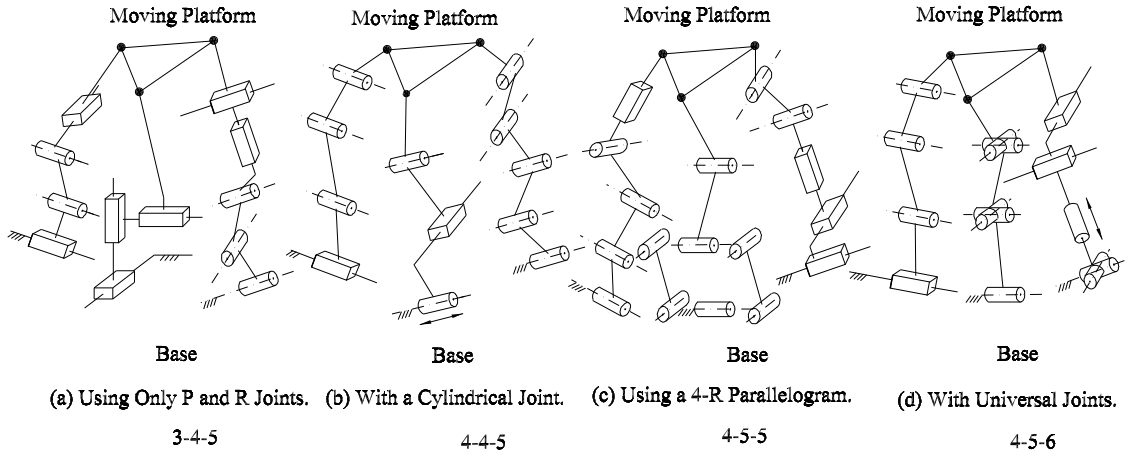

FIGURE 4.8. Constructions of asymmetrical three-legged TPMs.

serial kinematic chain composed of three prismatic joints, to represent the motion of the moving platform of a TPM. This artifact to produce the derivations simplifies the synthesis somewhat; however, the screw-theoretical basis inherent in this approach still leaves concepts that are not easy to follow.

Carricato and Parenti-Castelli (2003) presented a family of three-dof TPMs using vector operations. In their research, only revolute and prismatic joints are employed. By defining the axis vectors of different joints and according to some conditions examined, they investigated four cases and generated some possible TPM architectures. Although the theory is not hard to comprehend, the derivation and computation is tedious. Moreover, in that research the whole family of TPMs is not synthesized comprehensively. The situation is similar to the work of Di Gregorio (2002), where the condition is that the angular velocity and acceleration of the moving platform is zero. In that paper, only TPMs with five-dof legs are obtained.

The method proposed in this thesis, TPM synthesis based on displacement subgroups, is easy to follow and sufficient to generate any possible three-legged TPM architecture. As shown in the foregoing sections, similar conclusions have been obtained as with screw theory. The main advantage claimed for our method is its simpler

derivation. By designing kinematic chains according to their kinematic characteristics as described by displacement subgroups, synthesis is reduced to finding all the possible combinations of basic displacement subgroups. Moreover, this method avoids overlooking possible cases if the correct synthesis formula is utilized. The flowchart shown in Fig. 4.9 describes the synthesis procedure in a neat, compact way. The author believes that the displacement group concept can be regarded as a fundamental design tool and extended to the synthesis of many other mechanisms.

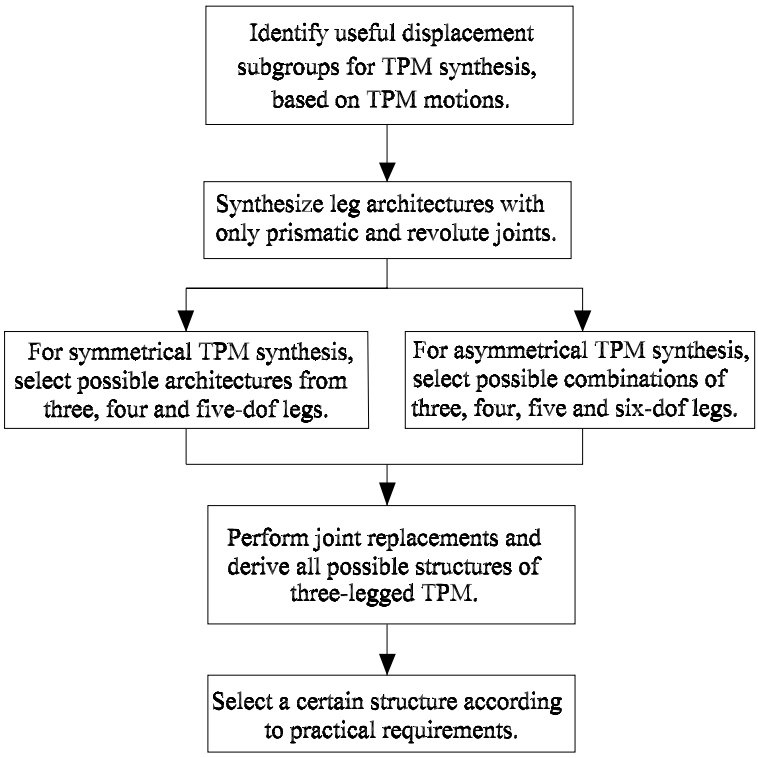

FIGURE 4.9. A flowchart of the proposed TPM synthesis procedure.

CHAPTER 5

TPM Kinematic Analysis with Geometric Graphs

In this chapter, the inverse and direct kinematic analyses of a TPM model with prismatic actuators are set forth. The approach to solve the TPM kinematics problem by intersecting corresponding geometric graphs is presented. This research work, named by the author as geometric kinematics, was first exposed in (Wei and Zsombor-Murray, 2004). The analyzed TPM model comes from the author's design in a course project, and has a similar, but not identical architecture as Orthoglide (Chablat and Wenger, 2003). Figure 5.1 shows the architecture of this TPM. Figure 5.2 displays the layout revealing that each leg of this TPM has one prismatic joint, two revolute joints and one Π joint, yielding a PRΠR structure, where the Π joint is a 4R parallelogram linkage. Three sliders move along three vertical rails attached to the base, forming three prismatic pairs. Taking one leg as an example, two opposite links in the four-bar linkage are respectively coupled to the slider and the moving platform by revolute joints. Each leg forms a Schönflies subgroup, thus having four dofs. A combination of three Schönflies subgroups forms the $\{T_3\}$ subgroup, which allows translations in all directions in three-dimensional space. Actually, this example belongs to a variation of the fourth case of class 2 in Subsection 3.3.2.

Section 5.1 analyzes the inverse kinematics of this TPM. Section 5.2 analyzes its direct kinematics. Section 5.3 discusses kinematics of variations to this TPM and draws some pertinent conclusions.

FIGURE 5.1. Model of the analyzed TPM.

5.1. The Inverse Kinematics Problem (IKP)

As shown in Fig. 5.3, the rails of the slides are schematically represented by three lines, L_1, L_2 and L_3. The four-bar linkage is represented by a line segment of length r_l. The fixed coordinate frame is defined so that the origin O is at the centre of the base triangle, with its x-axis intersecting line L_1 normally and its z-axis parallel to L_j $(j = 1, 2, 3)$. For the purpose of this example, each side of the base triangle is 2R and each side of the moving platform is 2r. Note that the value 2 chosen here simplifies the calculations. The three sliders are denoted by points A_1, A_2 and A_3, respectively, where the axis of the R-joint, which attaches the Π-joint to the centre line of the slider, intersects the latter normally. The three revolute joints coupled

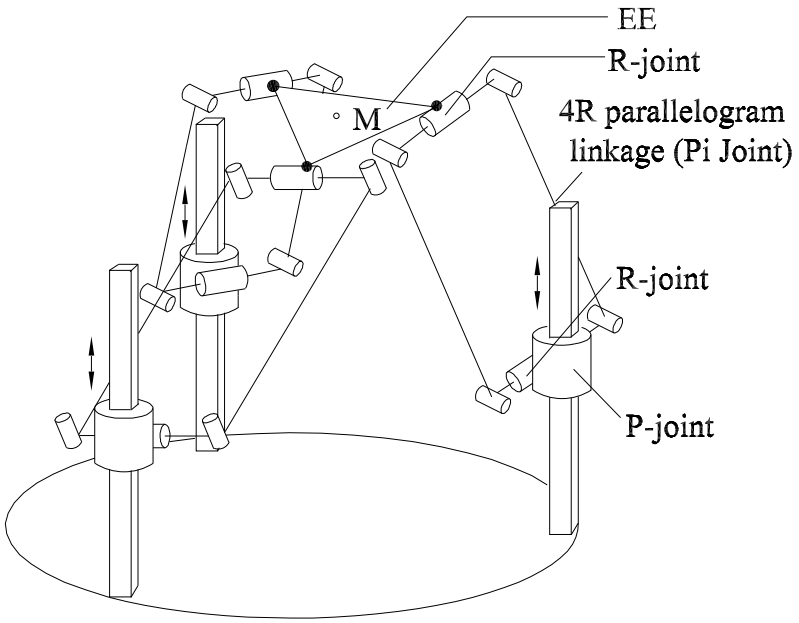

FIGURE 5.2. The kinematic structure of the analyzed TPM.

to the moving platform are represented by three points C_1, C_2 and C_3. To perform the IKP analysis, the coordinates of point M, the centre of the EE, are given as (x_M, y_M, z_M). The displacements of the three sliders, denoted as z_1, z_2 and z_3 in the z-direction, are unknowns.

Since a distinct characteristic of translational manipulators is that the moving platform may only exhibit translation in three directions, the directions of the segments directed from point M to points C_1, C_2 and C_3 do not change. Therefore, the coordinates of points C_1, C_2 and C_3 can be expressed as

$$\begin{aligned}
(x_{C1}, y_{C1}, z_{C1}) &= (x_M, y_M, z_M) + (\frac{2\sqrt{3}}{3}r, 0, 0) \\
(x_{C2}, y_{C2}, z_{C2}) &= (x_M, y_M, z_M) + (-\frac{\sqrt{3}}{3}r, r, 0) \\
(x_{C3}, y_{C3}, z_{C3}) &= (x_M, y_M, z_M) + (-\frac{\sqrt{3}}{3}r, -r, 0)
\end{aligned} \tag{5.1}$$

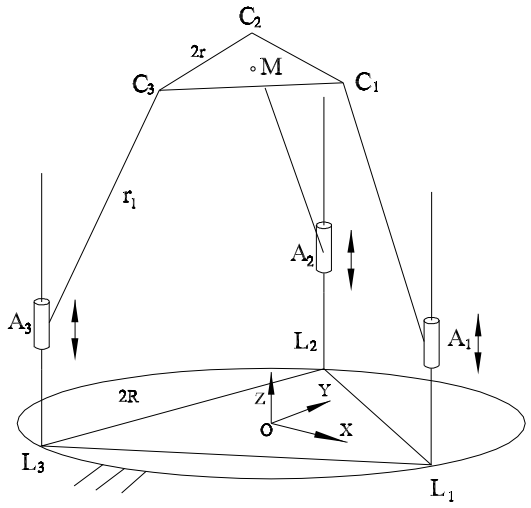

FIGURE 5.3. A simplified structure of the mechanism.

With respect to the point C_j, the four-bar linkage can perform two rotations, one about the axis of the R-joint at C_j, the other about the normal at C_j of the four-bar linkage plane, respectively. For example, when unconstrained, the workspace of a leg attached at C_j but detached from the slider is a sphere centred at C_j with a radius of r_l. Assume that a point B on the sphere surface has the homogeneous coordinates $\{w : x : y : z\}$. According to the sphere equation with its centre and radius known, we can derive the three equations.

$$\begin{aligned}
(x_{C1}w - x)^2 + (y_{C1}w - y)^2 + (z_{C1}w - z)^2 - r_l^2 w^2 = 0 \\
(x_{C2}w - x)^2 + (y_{C2}w - y)^2 + (z_{C2}w - z)^2 - r_l^2 w^2 = 0 \\
(x_{C3}w - x)^2 + (y_{C3}w - y)^2 + (z_{C3}w - z)^2 - r_l^2 w^2 = 0
\end{aligned} \tag{5.2}$$

Moreover, for the three lines L_i representing rails, we can write radial Plücker coordinates as

$$\begin{aligned} L_1 &: \{0:0:1:0:-\frac{2\sqrt{3}}{3}R:0\} \\ L_2 &: \{0:0:1:R:\frac{\sqrt{3}}{3}R:0\} \\ L_1 &: \{0:0:1:-R:\frac{\sqrt{3}}{3}R:0\} \end{aligned} \tag{5.3}$$

Now the problem at hand is to seek the intersections of spheres and lines as the possible displacements of the three sliders. These can be found as the solutions of a combination of the sphere equations and the radial line equations.

Here we take the sphere 1, centred at point C_1, and the line L_1 as an example to calculate the intersections. Since the point B is also on the radial line, we recall the constraint of a point on a line.

$$X_i = \sum_{j=0}^{3} P_{ij} b_j = 0 \tag{5.4}$$

After replacing the radial coordinates of the line L_1 by their equivalent axial counterparts, we obtain the second constraint, namely,

$$\begin{bmatrix} 0 & p_{23} & p_{31} & p_{12} \\ -p_{23} & 0 & p_{03} & -p_{02} \\ -p_{31} & -p_{03} & 0 & p_{01} \\ -p_{12} & p_{02} & -p_{01} & 0 \end{bmatrix} \begin{bmatrix} w \\ x \\ y \\ z \end{bmatrix} = \begin{bmatrix} 0 \\ 0 \\ 0 \\ 0 \end{bmatrix} \tag{5.5}$$

The values of x and y can be calculated from Eq. (5.5) as

$$\begin{aligned} x &= \frac{2\sqrt{3}}{3}R \\ y &= 0 \end{aligned}$$

Substituting the values of x and y into Eq. (5.2) yields

$$[(x_M + \frac{2\sqrt{3}}{3}r)w - \frac{2\sqrt{3}}{3}R]^2 + (y_M w)^2 + (z_M w - z)^2 - r_l^2 w^2 = 0 \tag{5.6}$$

which is a quadratic equation in terms of z. Solving this equation, two positions of the slider 1 are obtained

$$z_1 = \frac{-P + \sqrt{P^2 - 4Q}}{2}$$
$$z_2 = \frac{-P - \sqrt{P^2 - 4Q}}{2}$$

where

$$P = -2z_M w$$
$$Q = [(x_M + \frac{2\sqrt{3}}{3}r)w - \frac{2\sqrt{3}}{3}R]^2 + (y_M w)^2 + (z_M w)^2 - r_l^2 w$$

z_1 and z_2 are the inverse kinematics solutions for the displacements of slider 1.

Using the same method, the displacements of sliders 2 and 3 can be calculated as well. For each slider there are two solutions, the IKP of this structure admits eight possible solutions. In general, selection among these solutions is obvious, since the sliders do not descend beneath the base, i.e., complex solutions and solutions where $z < 0$ are deemed unacceptable.

5.2. The Direct Kinematics Problem (DKP)

In the DKP calculation, the displacement of the sliders are known, while the position of the moving platform is sought. Again, using the algebraic geometric method, the problem at hand can be easily solved.

First, we give the displacements of the actuators A_1, A_2 and A_3, namely, the coordinates of the sliders.

$$\begin{aligned} A_1 &: (\frac{2\sqrt{3}}{3}R, 0, z_1) \\ A_2 &: (-\frac{\sqrt{3}}{3}R, R, z_2) \\ A_3 &: (-\frac{\sqrt{3}}{3}R, -R, z_3) \end{aligned} \tag{5.7}$$

Similar to the IKP analysis outlined in Section 5.1, with respect to each slider, the movements of a point on the four-bar linkage are bound to a sphere. The point can

rotate about the axis of the revolute joint on the slider; the point can also rotate in the four-bar plane. So, again, an unconstrained point on the four-bar linkage moves on a sphere centred at point A_j. This allows us to derive three sphere equations. However, the sphere surface is only a possible position, of the revolute joint coupled to the moving platform, from which the displacements of the EE centre cannot yet be obtained. Notice that the distinct characteristic of a TPM applies to all its motions. The relative directional relation of EE's centre M and the three joints remains the same, so that allows us to move the centres of the four-bar sphere, A_1, A_2 and A_3, horizontally inward, by a distance of $2\sqrt{3}r/3$. Based on this, we can write the coordinates of the displaced sphere centres.

$$\begin{aligned} O_1 &: (\frac{2\sqrt{3}}{3}R, 0, z_1) - (\frac{2\sqrt{3}}{3}r, 0, 0) = (\frac{2\sqrt{3}}{3}(R-r), 0, z_1) \\ O_2 &: (-\frac{\sqrt{3}}{3}R, R, z_2) - (-\frac{\sqrt{3}}{3}r, r, 0) = (-\frac{\sqrt{3}}{3}(R-r), (R-r), z_2) \\ O_3 &: (-\frac{\sqrt{3}}{3}R, -R, z_3) - (-\frac{\sqrt{3}}{3}r, -r, 0) = (-\frac{\sqrt{3}}{3}(R-r), -(R-r), z_3) \end{aligned} \tag{5.8}$$

We assume that a point on the sphere centred at point O_j has the homogeneous coordinates of $\{w : x : y : z\}$; then, the sphere equation can be written as

$$(x_O w - x)^2 + (y_O w - y)^2 + (z_O w - z)^2 - r_l^2 w^2 = 0 \tag{5.9}$$

Hence, the three sphere equations can be derived.

$$(\frac{2\sqrt{3}}{3}(R-r)w - x)^2 + y^2 + (z_l w - z)^2 - r_l^2 w^2 = 0 \tag{5.10}$$

$$(-\frac{\sqrt{3}}{3}(R-r)w - x)^2 + ((R-r)w - y)^2 + (z_2 w - z)^2 - r_l^2 w^2 = 0 \tag{5.11}$$

$$(-\frac{\sqrt{3}}{3}(R-r)w - x)^2 + (-(R-r)w - y)^2 + (z_3 w - z)^2 - r_l^2 w^2 = 0 \tag{5.12}$$

Now, intersecting two pairs of the three spheres, we can derive two circles, and a line on the planes of the two circles yields two solutions on its intersection with any sphere. These are the two possible positions of the centre M of the moving platform when displacements of the input actuators are given.

Equations (5.10) through (5.12) are all quadratic. An easy way to solve them is to find the difference of two equation pairs, which yields two linear equations. Together with a sphere equation, these produce a quadratic univariate equation in, say x. The two solutions may be backsubstituted into the two linear equations, resulting in unique corresponding values of y and z. Thus, the position of the moving platform can be obtained.

Substracting Eq. (5.10) from Eq. (5.11) and Eq. (5.11) from Eq. (5.12) produces the two linear equations.

$$D_1 x_0 + E_1 y_0 + F_1 z_0 + G_1 = 0 \tag{5.13}$$

$$D_2 x_0 + E_2 y_0 + F_2 z_0 + G_2 = 0 \tag{5.14}$$

where $x_0 = x/w$, $y_0 = y/w$ and $z_0 = z/w$ are the Cartesian coordinates of point M, and

$$\begin{aligned} D_1 &= 2\sqrt{3}(R-r) \\ E_1 &= -2(R-r) \\ F_1 &= 2(z_1 - z_2) \\ G_1 &= (z_2^2 - z_1^2) \end{aligned}$$

$$\begin{aligned} D_2 &= 0 \\ E_2 &= 4(R-r) \\ F_2 &= 2(z_2 - z_3) \\ G_2 &= (z_3^2 - z_2^2) \end{aligned}$$

Solving the Eqs. (5.13) and (5.14) yields

$$\begin{aligned} x_0 &= \frac{1}{D_1}[\frac{E_1}{E_2}(F_2 z_0 + G_2) - F_1 z_0 - G_1] \\ y_0 &= -\frac{1}{E_2}(F_2 z_0 + G_2) \end{aligned}$$

Together with the equation of sphere 1, we have one quadratic equation, with z_0 as the unique variable. Solving this equation, we can obtain

$$z_0 = \frac{-I \pm \sqrt{I^2 - 4HJ}}{2H}$$

where

$$\begin{aligned}
H &= \frac{1}{D_1^2 E_2^2}(E_1F_2 - E_2F_1)^2 + \frac{F_2^2}{E_2^2} + 1 \\
I &= \frac{2}{D_1^2 E_2^2}(E_1F_2 - E_2F_1)(E_1G_2 - E_2G_1) + \frac{2F_2G_2}{E_2^2} - \frac{2}{3E_2}(E_1F_2 - E_2F_1) - 2z_1 \\
J &= \frac{1}{D_1^2 E_2^2}(E_1G_2 - E_2G_1)^2 + \frac{G_2^2}{E_2^2} + z_1^2 - r_l^2 - \frac{2}{3E_2}(E_1G_2 - E_2G_1) + \frac{4}{3}(R-r)^2
\end{aligned}$$

Now, we have obtained the z-axis coordinates of point M. Substituting z_0 into Eqs. (5.13) and (5.14), the two DKP solutions of this special TPM can be obtained.

$$\begin{aligned}
x_0 &= \frac{(E_1F_2 - E_2F_1)z_0 + (E_1G_2 - E_2G_1)}{D_1E_2 - D_2E_1} \\
y_0 &= \frac{(D_1F_2 - D_2F_1)z_0 + (D_1G_2 - D_2G_1)}{D_2E_1 - D_1E_2} \\
z_0 &= \frac{-I \pm \sqrt{I^2 - 4HJ}}{2H}
\end{aligned} \tag{5.15}$$

5.3. TPMs with Arbitrary P-Joint Translation Directions

Now we consider the TPM example introduced in the foregoing context. Its particular architecture of slider and four-bar linkage leg layout reduces the IKP analysis to the intersections between spheres and radial lines. Similarly, the DKP analysis is formulated as intersections among three spheres. Now the approach is restated in a more general way. When solving the inverse kinematics problem, with the EE position given, we can locate the points connecting legs and the EE. For each leg, there are two spatial geometric graphs, one located on the fixed frame (FF), the other on the EE. Intersections of these two geometric graphs yield the possible solutions of the IKP. In direct kinematics, the actuated joint displacements are given, and the position of the link coupled to the FF is to be determined. What we seek are the intersections of the workspace of the links coupled to the EE, namely, the possible

solutions of the DKP. Such a geometric thinking makes the TPM kinematics problem easy to visualize and to explain.

Other TPMs, with quite different architectures, are solved with similar methods. Clavel's Delta robot is a good example, whose kinematics problems are treated as intersections between circles in the IKP and spheres in the DKP (Zsombor-Murray, 2001). Now, let us consider the Orthoglide (Chablat and Wenger, 2003), as shown in Fig. 4.7. It is apparent that this manipulator also has three legs, in this case driven by three prismatic joints. Each leg is a PRΠR serial array that is the same as the architecture analyzed in this chapter. The Orthoglide is subject to the same kinematics analysis method. Note that the directions of translation of the three prismatic joints in Orthoglide are orthogonal; what changes in the solution procedure are just the sets of Plücker coordinates of the three lines A_jB_j, which are geometrically equivalent to the three parallel rails of the TPM analyzed in Sections 5.1 and 5.2. The situation is also the same if the three lines have arbitrary directions.

CHAPTER 6

Applicability Investigation of the Proposed Approach

In this chapter, the applicability of the approach proposed in Chapter 5 is examined. Section 6.1 employs Tsai's CPM (2003) as an example to be analyzed and derives its kinematics solutions. Section 6.2 discusses the general applicability of the approach to a class of TPMs.

6.1. Kinematic Analysis of Tsai's CPM

We recall Fig. 4.4. Tsai (2003) proposed the CPM that employs only revolute and prismatic joints to achieve translational motion of the moving platform. CPM has two actuation options, linear actuation and rotary actuation. Its kinematic structure is reproduced as shown in Fig. 6.1.

Now we start to solve kinematic problems of CPM with linear actuation.

6.1.1. Linear Actuation. For the linear actuation, a linear actuator drives the prismatic joint in each leg, while all revolute joints are passive. Notice that the jth (j=1,2,3) leg only moves in the plane defined by links A_jM_j and M_jB_j, as shown in Fig. 6.1, and the prismatic actuators provide motion normal to their respective planes.

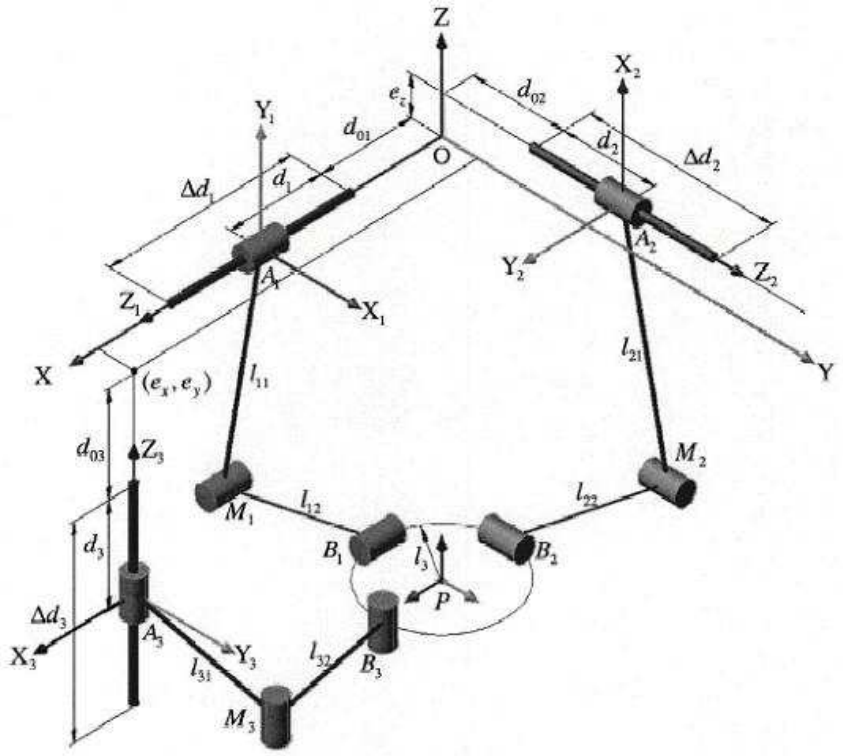

FIGURE 6.1. Kinematic architecture of Kim and Tsai's CPM (2003).

For the inverse kinematics, one can define each plane $A_jM_jB_j$ by its normal and any incident point P. The normal has the same direction as the translation of points provided by each prismatic joint, and the point P is given a-priori. Then, the intersection of each plane and its corresponding line, which is directed along the motion of the linear actuator, gives the solution of the IKP.

For the direct kinematics, each plane is defined by the normal and the position of each slider. The intersection of three planes determines the position of point P, the solution of the DKP.

Actually, due to the special structure of Tsai's CPM, its kinematics for linear actuation is trivial and it admits a one-to-one correspondence between the positions of the actuators and that of EE, like the serial x-y-z table of a milling machine.

6.1.2. Rotary Actuation. If rotary actuation is chosen, three rotary actuators drive the revolute joints located at A_1, A_2 and A_3, with all other joints remaining passive.

For the IKP, as introduced in Subsection 6.1.1, when the position of the EE is given, say the coordinates of point P, we can determine the position of some point on the moving element of each prismatic joint, namely the coordinates of point A_j, as the intersection of the plane and the actuator piston centre line,

$$\begin{aligned} A_1 &: (p_x, 0, 0) \\ A_2 &: (0, p_y, 0) \\ A_3 &: (x_0, y_0, p_z) \end{aligned}$$

where (p_x, p_y, p_z) are the coordinates of point P, and x_0 and y_0 are the coordinates of the projection of axis Z_3 on X-Y plane; therefore, they are constants.

Moreover, the coordinates of point B_j are obtained as

$$\begin{aligned} B_1 &: (p_x, p_y + b_1, p_z) \\ B_2 &: (p_x + b_2, p_y, p_z) \\ B_3 &: (p_x + b_3, p_y, p_z) \end{aligned}$$

where $b_j (j = 1, 2, 3)$ is the offset between the positions of points P and B_j.

For the jth leg, we obtain two circles, centred at points A_j and B_j, with radii l_{j1} and l_{j2}, respectively, as shown in Fig. 6.2.

Taking the first leg as an example, the two circle equations are obtained as

$$\begin{cases} y^2 + z^2 = l_{11}^2 \\ x = p_x \end{cases}$$

$$\begin{cases} (y - p_x - b_1)^2 + (z - p_z)^2 = l_{12}^2 \\ x = p_x \end{cases}$$

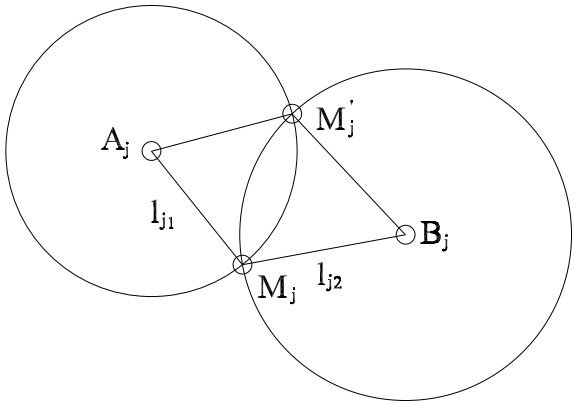

FIGURE 6.2. Geometric representations for one leg.

The two circles intersect at two points, denoted by coordinates (p_x, y_1, z_1) and (p_x, y_2, z_2).

Then, the actuation angles are derived as

$$\theta_{11} = \arctan(\frac{z_1}{y_1})$$
$$\theta_{12} = \arctan(\frac{z_2}{y_2})$$

For each leg, there are two possible solutions for the IKP. Therefore, with rotary actuation, Tsai's CPM admits at most eight inverse-kinematics solutions.

For the direct kinematics, the actuation angles are given, and the position of point P is sought. In the case at hand, point A_j can be located anywhere on the actuator axis due to the motion of the prismatic joint. Therefore, we can only determine the position of point M_j on a line parallel to its corresponding actuator axis with a distance l_{j1}, and the orientation of the perpendicular of the two lines can be determined by the actuator joint angle. Due to the kinematic characteristic of the EE, we move point M_j horizontally inward to point N_j, with a distance b_j, the positional offset of points B_j and P, as shown in Fig. 6.3. Consequently, the three points B_1, B_2 and B_3 converge at point P.

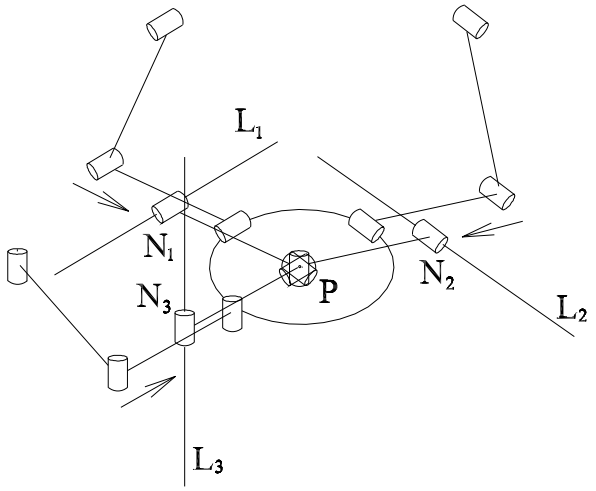

FIGURE 6.3. Displaced rotating axes and convergence on point P.

Now if we take the line L_j as the axis of rotation, and the link length l_{j2} as the radius, we obtain three cylinders of revolution, whose intersection determines the position of the EE. Since a cylinder of revolution is a quadric, intersecting three of them admits at most eight distinct real solutions. In practice, some pairs may turn out to be complex. Therefore, eight different configurations are theoretically possible for the direct kinematics of this TPM. The same results were also reported by Kim and Tsai (2003).

6.2. Applicability Investigation

Again, as stated in Section 4.1, by employing joint replacements we can obtain a class of TPMs with different structures. Table 6.1 shows some possible combinations of P, R and Π joints to form the leg architecture of a three-legged symmetrical TPM. The corresponding kinematic geometry representations are summarized in the same table. For the class of TPMs listed in Table 6.1, the corresponding leg architectures are shown in Fig. 6.4. Note that in Table 6.1, cylinder stands for cylinder of revolution; (1) and (2) represent linear actuation and rotary actuation, respectively.

TABLE 6.1. Geometric representations and the maximum number of solutions for a class of TPMs.

Leg architecture	**IKP**		**DKP**	
	Geometry elements	No. of Sols	Geometry elements	No. of Sols
P R Π R	Sphere & Line	8	Spheres	2
P Π R R	Circle & Cylinder	8	Bohemian domes	64
P R R R (1)	Plane & Line	1	Planes	1
P R R R (2)	Circle & Circle	8	Cylinders	8
P Π Π R	Plane & Line	1	Plane	1
R R Π R	Sphere & Circle	8	Spheres	2
R Π R R	Circle & Sphere	8	Bohemian domes	64
R Π Π R	Plane & Plane	1	Planes	1

Here the Bohemian dome (Bonev, 2002) is introduced as follows. Given a circle C_1 and plane E perpendicular to the plane of C_1, we move a second circle C_2 through space so that the centre of C_2 always lies on the circumference of C_1, and C_2 remains parallel to E. Then C_2 sweeps out the Bohemian dome. A Bohemian dome differs from a torus in that the rotating circle of a torus changes its orientation in a turn; however, the orientation of the rotating circle of a Bohemian dome remains fixed. Figure 6.5 depicts the lower half of a Bohemian dome, which is a fourth-order surface. Therefore, an intersection of three Bohemian domes with arbitrarily skewed axes may, in theory, yields a maximum of 64 solutions for PΠRR and RΠRR leg architectures.

From the examples listed in Table 6.1, it is clear that by using geometric elements to denote the workspace of different links, one can find all possible kinematics solutions by intersecting the related spatial surfaces. This geometric thinking provides an effective and fast way to comprehensively analyze the inverse and direct kinematics of three-legged symmetrical TPMs.

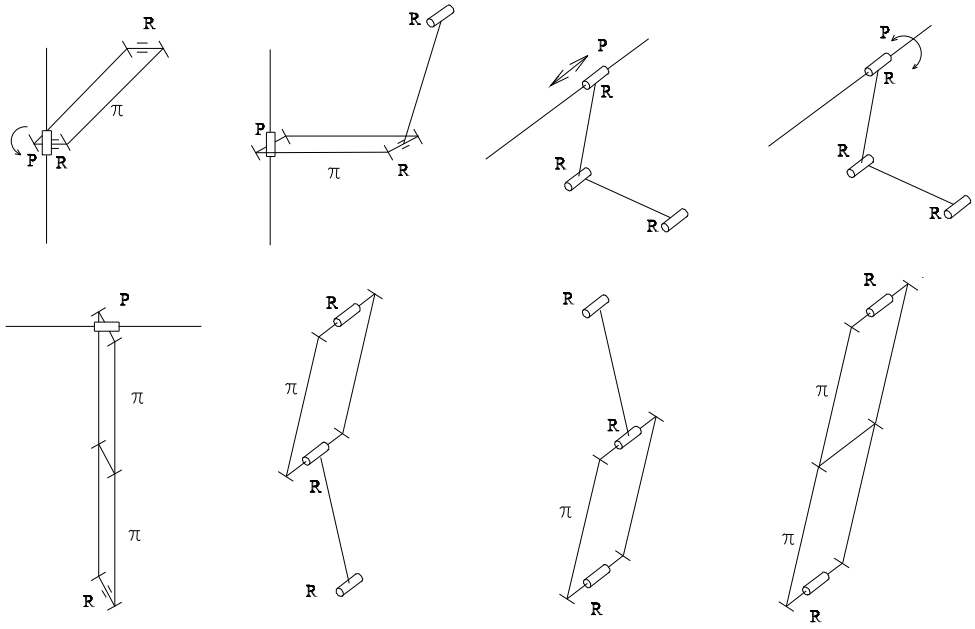

FIGURE 6.4. Leg architectures for the class of TPMs listed in Table 6.1.

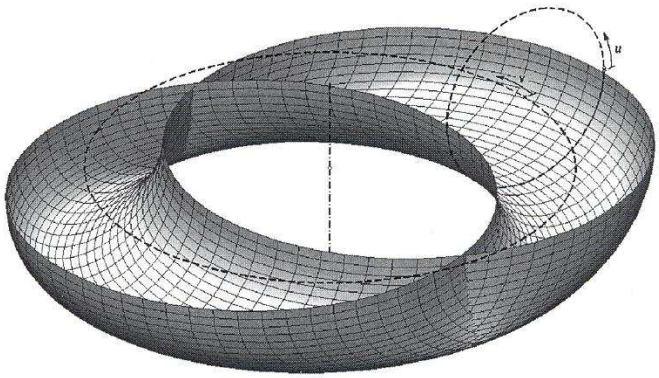

FIGURE 6.5. The lower half of a Bohemian dome surface.

CHAPTER 7

Conclusions

7.1. Conclusions

In this thesis, a comprehensive analysis of three-legged TPMs was presented, including both type synthesis and inverse and direct kinematics.

For the TPM type synthesis, DGT is the theoretical basis. With twelve displacement subgroups, the synthesis procedure is carried out in two steps: first, leg-architecture synthesis; second, constructing the entire TPM. Based on the correct synthesis formula, type synthesis of TPMs can be simplified to a permutation and combination problem. Finally, the whole family of three-legged symmetrical TPMs composed of prismatic and revolute joints, as well as some three-legged asymmetrical TPMs, are proposed. To the author's knowledge, this work is original in systematically synthesizing TPM architectures with DGT.

For the TPM kinematic analysis with geometric graphs, a specific three-legged symmetrical TPM with PRΠR leg architecture was analyzed. By using spheres and lines to denote the workspace of its leg links for the inverse kinematics, and using three spheres to denote that for the direct kinematics, the kinematics solutions are obtained by intersecting the corresponding geometric graphs. Finally, the applicability of this approach was examined by applying it to a class of TPMs with joint replacements. When the kinematics problem is solved by finding geometric representations of the

workspace of leg links, it is easy to formulate a set of constraint equations that greatly simplify the solution procedure.

7.2. Suggestions for Future Research

Besides TPMs, there are many PKMs, and mechanical systems in general which can be synthesized based on DGT. If the synthesis of a mechanism is performed by considering its motion characteristics and finding the corresponding subgroup representations, fast and comprehensive results may be obtained.

The kinematic analysis approach using geometric graphs can be further investigated for the whole family of TPMs, as synthesized in this thesis. It will be a lengthy but straightforward procedure. The idea of denoting link workspace with geometric graphs can be extended to other problems related to kinematics and dynamics of mechanical systems as well.

REFERENCES

Angeles, J., 2003, Lecture Notes of MECH 541 Kinematic Synthesis, Department of Mechanical Engineering, McGill University, 178 pp.

Angeles, J., 2004, "The Qualitative Synthesis of Parallel Manipulators", *ASME Journal of Mechanical Design*, Vol. 126, pp. 617-624.

Bonev, I. A., 2002, "Geometric Analysis of Parallel Mechanisms", Ph.D Thesis, Université Laval, Québec (Québec), Canada.

Carricato, M. and Parenti-Castelli, V., 2002, "Singularity-free Fully-isotropic Translational Parallel Mechanisms", *The International Journal of Robotics Research*, Vol.21, No.2, pp. 161-174.

Carricato, M. and Parenti-Castelli, V., 2003, "A Family of 3-DOF Translational Parallel Manipulators", *ASME Journal of Mechanical Design*, Vol. 125, pp. 302-307.

Carricato, M. and Parenti-Castelli, V., 2003, "Position Analysis of a New Family of 3-DOF Translational Parallel Manipulators", *ASME Journal of Mechanical Design*, Vol. 125, pp. 316-322.

Chablat, D. and Wenger, P., 2003, "Architecture Optimization of a 3-DOF Translational Parallel Mechanism for Machining Applications, the Orthoglide", *IEEE Transactions on Robotics and Automation*, Vol. 19, No. 3, pp. 403-410.

Clavel, R., 1988, "Delta, a Fast Robot with Parallel Geometry", 18*th International*

Symposium on Industrial Robots, Sydney, Australia, pp. 91-100.

Di Gregorio, R., 2002, "Translational Parallel Manipulators: New Proposals", *Journal of Robotic Systems*, Vol. 19, No. 12, pp. 595-603.

Hervé, J. M., 1978, "Analyse Structurelle des Mécanismes par Groupe des Déplacements", *Mechanism and Machine Theory*, Vol. 13, pp. 437-450.

Hervé, J. M. and Sparacino, F., 1991, "Structural Synthesis of 'Parallel' Robots Generating Spatial Translation", *Proc. of the 5th International Conference on Advanced Robotics*, Pisa, Italy, June 19-22, Vol. 1, pp. 808-813.

Hervé, J. M., 1999, "The Lie Group of Rigid Body Displacements, a Fundamental Tool for Mechanisms Design", *Mechanism and Machine Theory*, Vol. 34, No. 5, pp. 719-730.

Kim, H. S. and Tsai, L. W., 2003, "Design Optimization of a Cartesian Parallel Manipulator", *ASME Journal of Mechanical Design*, Vol. 125, pp. 43-51.

Kohli, D., Lee, S. H., Tsai, K. Y., and Sandor, G. N., 1988, "Manipulator Configurations Based on Rotary-Linear (r-l) Actuators and Their Direct and Inverse Kinematics", *ASME Journal of Mechanisms, Transmissions, and Automation in Design*, Vol. 110, pp. 397-404.

Kong, X. and Gosselin, C. M., 2002, "Kinematics and Singularity Analysis of 3-CRR 3-DOF Translational Parallel Manipulators", *The International Journal of Robotics Research*, Vol. 21, No. 9, pp. 791-798.

Kong, X. and Gosselin, C. M., 2004, "Type Synthesis of 3-DOF Translational Parallel Manipulators Based on Screw Theory", *ASME Journal of Mechanical Design*, Vol. 126, pp. 83-92.

Kong, X. and Gosselin, C. M., 2004, "Type Synthesis of 3-DOF Translational Parallel Manipulators Based on Screw Theory and a Virtual Joint", *Proc. of Romansy* 2004,

Montreal, Quebec, Canada, June 14-18.

Li, Q., Huang, Z. and Hervé, J. M., 2004, "Type Synthesis of 3R2T 5-DOF Parallel Mechanisms Using the Lie Group of Displacements", *IEEE Transactions on Robotics and Automation*, Vol. 20, No. 2, pp. 173-180.

Pierrot, F., Fournier, A. and Dauchez, P., 1991, "Toward a Fully Parallel 6 DOF Robot for High-speed Applications", *Proc. IEEE International Conference on Robotics and Automation*, Vol. 2, pp. 1288-1293.

Stewart, D., 1965, "A Platform with Six Degrees of Freedom", *Proc. of Institute of Mechanical Engr.*, Vol. 180, pp. 371-386.

Tahmasebi, F. and Tsai, L. W., 1994, "Six-degree-of-freedom Parallel Minimanipulator with Three Inextensible Limbs", U.S. Patent, No. 5,279,176.

Tsai, L. W., Walsh, G. C. and Stamper, R. E., 1996, "Kinematics of a Novel Three DOF Translational Platform", *Proc. of the* 1996 *IEEE International Conference on Robotics and Automation*, Minneapolis, Minnesota, pp. 3446-3451.

Tsai, L. W. and Joshi, S., 2001, "Comparison Study of Architectures of Four 3 Degree-of-freedom Translational Parallel Manipulators", *Proc. of the* 2001 *IEEE International Conference on Robotics and Automation*, Seoul, Korea, pp. 1283-1288.

Wei, W. and Zsombor-Murray, P., 2004, "Translational Parallel Manipulator Kinematics Using Algebraic and Projective Line Geometry Elements", *Proc. of the* 2004 *CCToMM Symposium*, 2004 *CSME Forum*, June 1-4, London, Ontario, Canada, pp. 44-52.

Zsombor-Murray, P., 1996, "Points, Planes and Lines", *Engineering Design Graphics Journal*, Vol. 60, No. 2, pp. 5-14.

Zsombor-Murray, P., 1998, "Normed Dual Quaternions for Computation", Lecture

Notes, TU-Graz Institute for Geometry, 13 pp.

Zsombor-Murray, P., 2001, "Kinematic Analysis of Clavel's 'Delta' Robot", *Proc. of the* 18*th Canadian Congress of Applied Mechanics*, St. John's, Canada, June 3-7, pp. 303-304.

Document Log:

Manuscript Version 2 — April, 2005

Typeset by $\mathcal{AMS}$-LaTeX — 8 April 2005

Wei Wei

Centre for Intelligent Machines, McGill University, 3480 University St., Montréal (Québec) H3A 2A7, Canada, *Tel.* : (514) 398-5856

E-mail address: weiwei@cim.mcgill.ca

Typeset by $\mathcal{AMS}$-LaTeX